

# 3. MACHINE COMPONENTS, HEAT TRANSFER AND STRAND SOLIDIFICATION

This chapter gives details of the main components of the casting machine and includes the mould, the strand support systems, the secondary cooling arrangements, strand straightening and strand withdrawal. In each case consideration is given to design principles and, in particular, the quantification of heat transfer in various parts of the machine and which is fundamental to the control of strand solidification. Additionally, methods will be described which have provided heat transfer data which can be used in various computer simulation models and to enable the design of systems and methods to control the solidification process. The computer simulation models dealing with mould technology, strand solidification and strand geometry will also be described in some detail.

The effects of these parameters, along with factors such as steel chemistry, on the presence of defects in the as-cast semis will be described in Chapter 4. This applies to both internal and surface defects.

## 3.1 Mould Technology

### 3.1.1 Mould Design Details

The mould is the only mechanical part of a caster that is exposed to molten steel. It is probably the most important part of the machine and has to operate under severe conditions. It needs to create a homogeneous shell by efficient uniform heat transfer. The mould also needs to be long lasting, be capable of rapid change of section sizes, and require the minimum of maintenance effort.

Continuous casting moulds are all cooled by high quality water, often demineralised, supplied from a recirculating system. The design and fail safe systems are usually arranged to provide a minimum water flow velocity in the cooling channels of 8 m/sec. Moulds are invariably tapered internally to accommodate contraction of the steel but the amount of taper depends on the section sizes and casting speeds involved.

Figure 3.1 shows the basic construction of a billet (a), bloom (b) and slab mould (c) respectively. The copper moulds are contained by steel backing

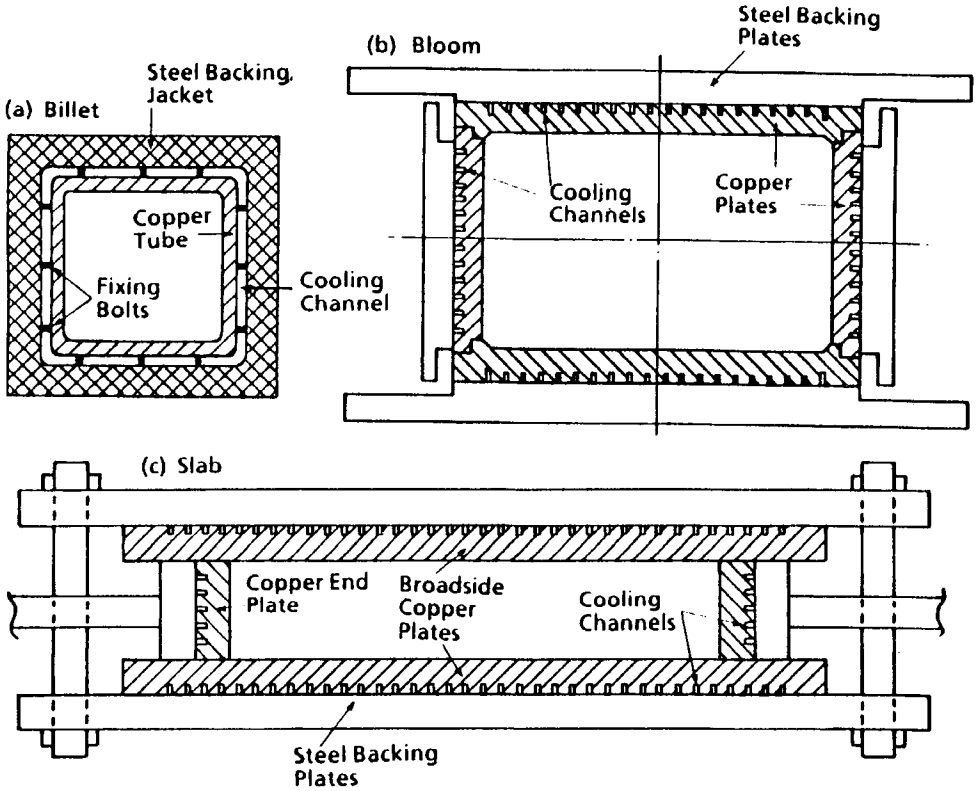


Figure 3.1 Mould constructions for billet, bloom and slab casters.

plates with water inlet and outlet manifolds at the bottom and top of the mould respectively.

The water cooling grooves are machined in the back of the copper plates from top to bottom in slab and bloom moulds the dimensions of these being about 15 mm deep and 5 mm wide. In billet moulds the water channel is usually a parallel gap between the tubular copper mould and the backing plate.

To ensure a thin boundary layer at the copper surface and hence no nucleate boiling, a high Reynolds number is required in these water cooling grooves which results in a need for the water velocities being greater than 8 m/sec.

The following are the two main mould types. These are:

**Tubular Moulds.** These are frequently used for casting small sections such as billets. The copper tube is surrounded by the water cooling jacket and, although easily deformed, the tube can be quickly exchanged or straightened. The maximum practical size is about 230 mm square, or 430 mm diameter for rounds castings but they are normally less than 200 mm

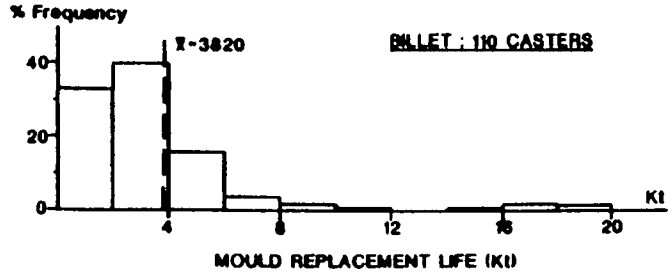
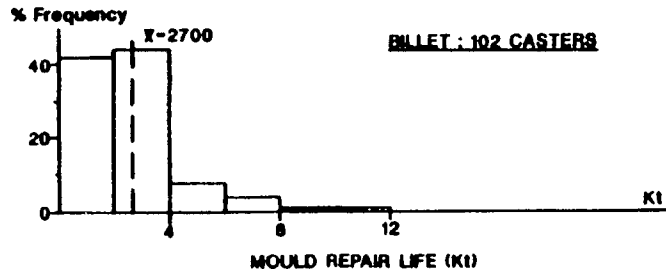
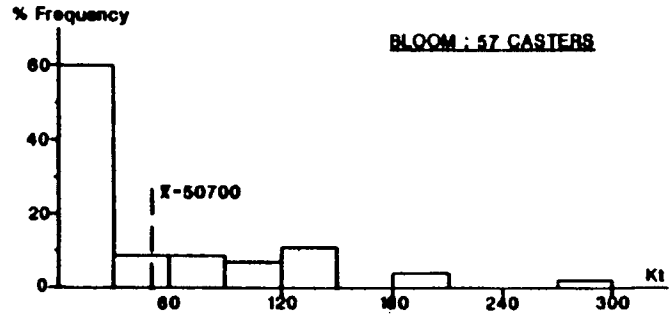
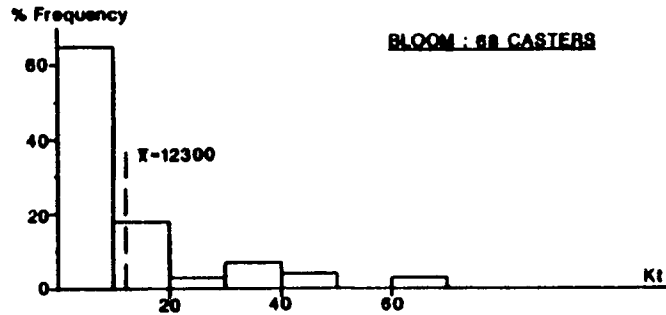
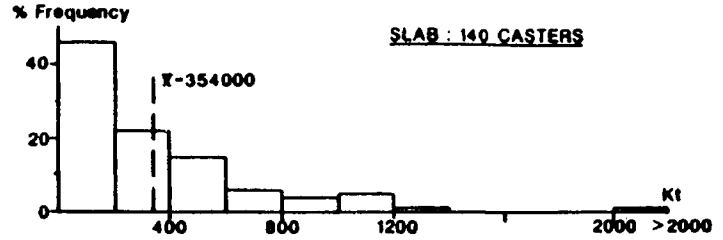
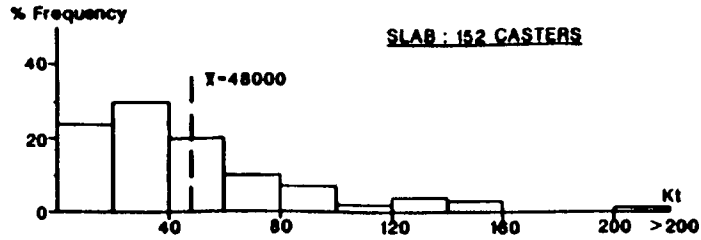


Figure 3.2 Mould lives for billet, bloom and slab casters.

across. The larger sizes have greater wall thicknesses of about 20 mm and on small sizes

**Plate Moulds.** These are assembled from four copper plates of 40 to 60 mm thick. The cold faces are grooved and covered with a steel backing plate. The cooling water passes through these grooves or, in an alternative design, through circular cooling channels machined in the copper. These moulds usually enable the narrow faces to be adjusted for different widths and these mechanisms can in some cases now be operated during casting (Section 3.1.1.4).

The copper plates in bloom and slab moulds are usually between 50 and 60 mm thick when new and about 40 mm thick at the end of their lives. Usually several machinings of the face are carried out during the plate life. Figure 3.2 shows the distribution of heats cast between machinings and for the total lives of slab, bloom and billet moulds respectively.<sup>1</sup>

#### *3.1.1.1 Mould Length*

The normal mould length was, until recently, 700 mm, but the range extends from 500 to 1,200 mm. The most recent trend has been towards 900 mm moulds to provide an increased solidified thickness at the mould outlet when casting at higher speeds.

#### *3.1.1.2 Mould Materials*

The mould material must rapidly transmit the heat from the solidified steel to the cooling water and hence good thermal conductivity is essential. Copper and copper alloys are invariably used but it is necessary to minimise distortion from thermal stress. Silver, chromium and zirconium alloying additions are used because of their improved high temperature properties;<sup>2</sup> Table 3.1 and Figure 3.3 give details. In some cases, the working face of the mould is plated to minimise wear. This is claimed to reduce star cracks formed when copper adheres to the solidified shell but many plants, particularly in Europe, operate successfully without plating.

Various methods of plating the copper with nickel and chromium have been developed. One technique uses a thick layer so the mould can be re-used after surface dressing. Other techniques taper the coating or use a two stage plating method, the intention being to minimise wear at the lower part of the mould. Another technique uses nickel iron plating and the increased hardness doubles the wear resistance. Mould plating is most common in Japan and finds only limited application elsewhere.

#### *3.1.1.3 Mould Oscillation*

The original idea of a reciprocating motion to prevent sticking between the shell and the mould is attributed to Junghans, see Section 1.1. With a few

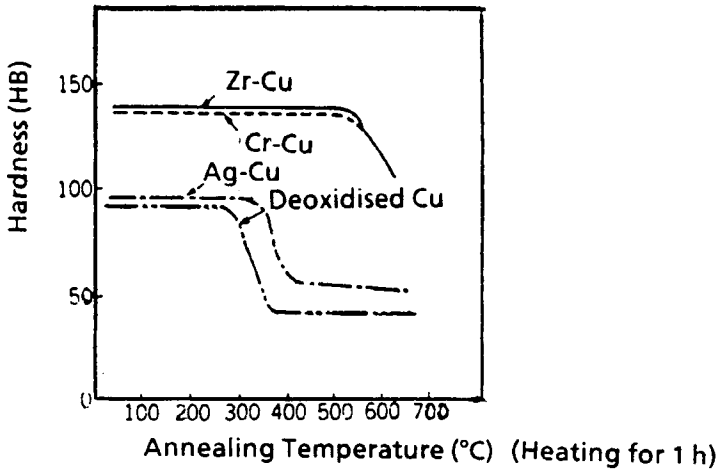


Figure 3.3 Softening resistance of copper alloys.

Table 3.1 Copper specifications

Chemical composition		Mechanical properties (minimum)				Electrical conductivity
Cu	Others	Tensile strength	0.2% proof strength	Elongation	Hardness	%IACS
(%)	(%)	(N/mm <sup>2</sup> )	(N/mm <sup>2</sup> )	(%)	(HB)	(20°C)
99.9		200	40	40	45	98
(Cu + Ag) 99.9	Ag 0.07–0.12	250	200	10	80	98
(Cu + Ag) 99.9	P 0.004–0.915 Ag 0.07–0.12	250	200	15	80	85
98.0	Cr 0.5–1.5	350	280	10	110	80
98.0	Cr 0.5–1.5 Zr 0.08–0.30	350	280	10	110	70
98.0	Cr 0.5–1.5 Zr 0.08–0.30	300	240	15	100	70

exceptions, the mould oscillation cycle is sinusoidal but in every case the downward velocity exceeds the casting speed for part of the cycle. During this time, (termed the negative strip time or heal time), sticking between the mould and the shell is overcome.

Mould oscillation is essential for the elimination of breakouts and under carefully controlled conditions the breakout rate can be virtually zero. The movement for mould oscillation is derived from a motor driven cam but

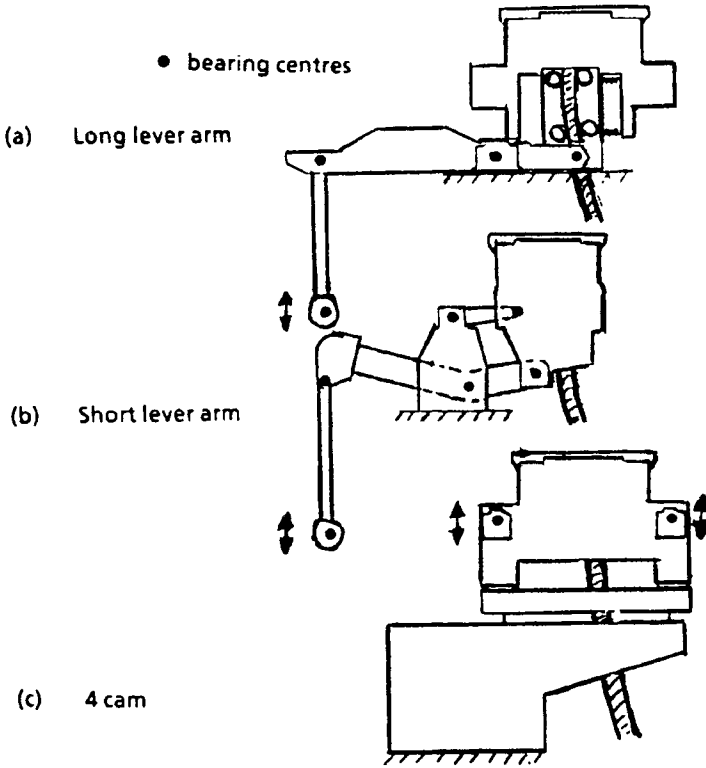


Figure 3.4 Mould oscillation mechanisms.

hydraulic devices have been developed. The design of the structure, bearings and lever arms is critical since the stroke length must remain equal at different points on the mould and only very small horizontal or radial movements of less than 0.2 mm can be tolerated. There are several design principles used such as direct cam drive, short or long lever arm or, more recently, hydraulic movement and some of them<sup>1</sup> are illustrated in Figure 3.4.

For best results the mounting points of the oscillation system should be separated from the casting floor and machine frame. Defective oscillation will result in increased breakout rate and surface defects on the strand.

Recent work has shown that there can be significant improvements to surface quality by operating with small heel times. This is usually achieved with small stroke lengths, down to 4 mm on slab machines<sup>3</sup> and down to 8 mm on billet machines and oscillation frequencies of 200 cycles/minute (cpm) or greater compared to the more usual 100 or 120 cpm. These higher frequencies and small stroke lengths, have shown benefits on some stainless steel casters and are becoming more common

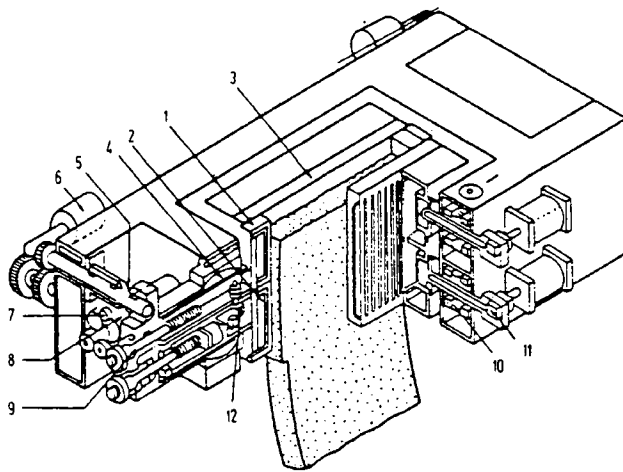
elsewhere, and place a greater demand on the design and upon the engineering standards for trouble free operation. More details of how the oscillation conditions affect as-cast quality will be given in Section 4.2.3.3

### 3.1.1.4 Variable Width Moulds

Over the last decade mould width changing during casting on slab machines has been established in a response to the demand for different slab widths without interruption of a sequence cast. The technique is applied in many current slab casters. A maximum width changing speed of 200 mm/min has been achieved by using a carefully chosen sequence of moving the narrow plates.<sup>4</sup>

The variable width is achieved by careful movement of the narrow faces which are power adjusted inwards or outwards during the casting process. The adjustment is made over a period of time and results in a tapered slab which may need special attention during reheating. Figure 3.5 shows the main components required for such adjustments.<sup>5</sup>

It is critical during the width change that the taper of the end plate is accurately controlled, the taper varying as the width is changed.



#### Mould construction:

- 1 - Top narrow faces
- 2 - Bottom narrow faces
- 3 - Broad faces

#### Taper adjustment system:

- 4 - Cage with rotary segment
- 5 - Cam
- 6 - Drive

#### Width adjustment and measuring system:

- 7 - Position indicator (pulse generator)
- 8 - Positioning motor
- 9 - Spindle

#### Mould clamping system:

- 10 - Release mechanism for width change
- 11 - Mould clamping device for casting
- 12 - Narrow face locking mechanism

Figure 3.5 Width adjustable mould with horizontally split narrow faces.



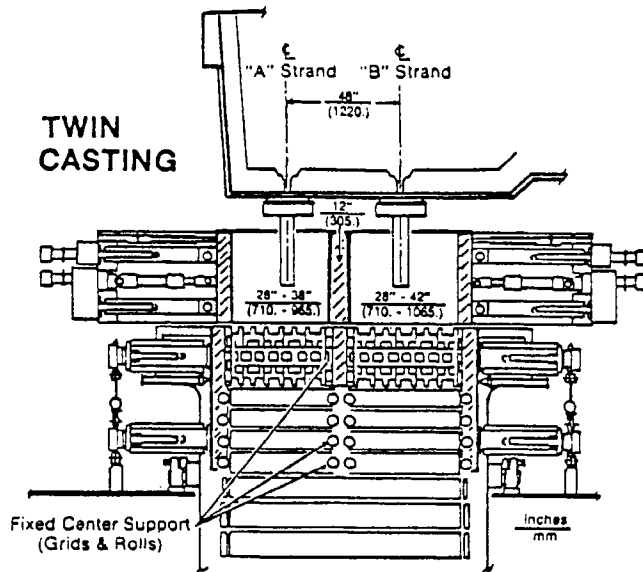


Figure 3.7 Sectional view of twin mould slab casting.

taking place during the continuous casting of steel. It is fundamental that the mould extracts heat from the steel in as uniform a manner as possible with some degree of control. The surface quality of the cast semi is very dependent on mould parameters since this is where the surface is formed and can, therefore, be the source of many surface defects. Uniform heat transfer also helps to avoid breakouts.

Further details of the defects and how they can be related to certain mould parameters are given in Chapter 4. Figure 3.8 shows the temperature distribution between the solidifying steel and the cooling water.<sup>7</sup>

The heat flux  $Q$  is given by:

$$Q = h_{ss} (T_{ss} - T_{hf}) = \frac{K}{D} (T_{hf} - T_{cf}) = h_{cf} (T_{cf} - T_{bw}) \text{ Kw/m}^2$$

where:

$h_{ss}$  = heat transfer coefficient from the face of the solidifying steel (kW/m<sup>2</sup> K)

$T_{ss}$  = temperature of the outer face of the solidifying steel (°C)

$T_{hf}$  = copper 'hot face' temperature (°C)

$T_{cf}$  = copper 'cold face' temperature (°C)

$K$  = thermal conductivity of copper (kW/m K)

$h_{cf}$  = heat transfer coefficient of the 'cold' copper face (kW/m<sup>2</sup> K)

$T_{bw}$  = bulk temperature of the cooling water (°C)

$D$  = thickness of copper (m)

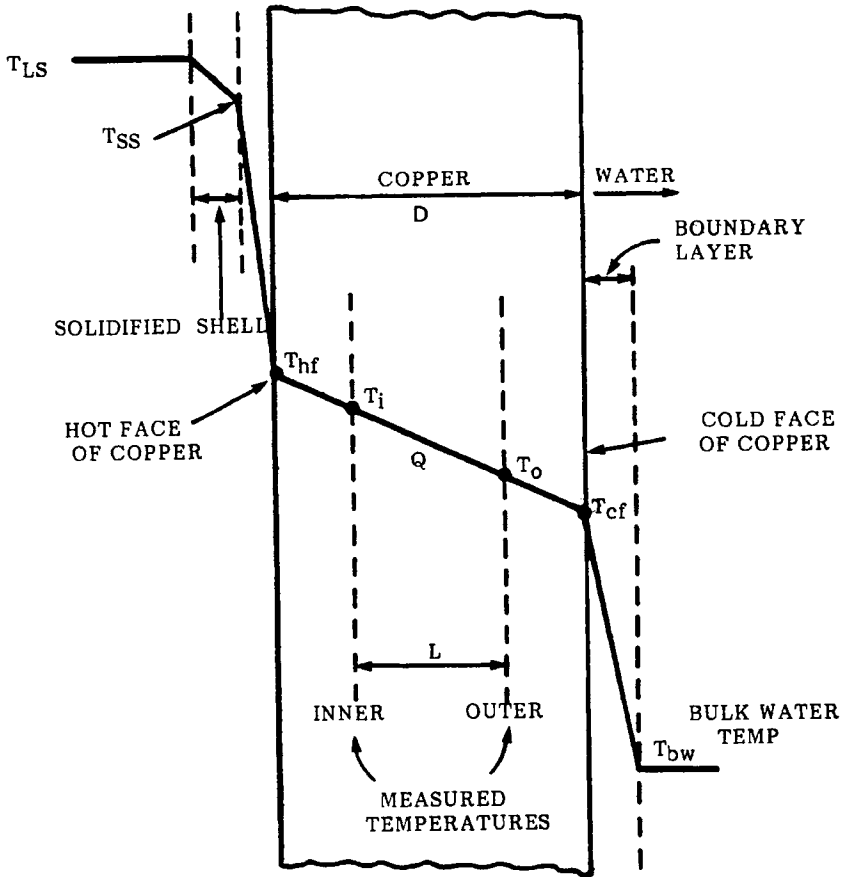


Figure 3.8 Temperature distribution between steel and cooling water.

From the liquid steel temperature in the mould, there is a temperature drop across the solidifying skin which will be discussed more fully in Section 3.4.1. The interface between the steel shell and the hot face of the mould wall incorporates the film of lubricant and any gaps which form and this component of the heat transfer represents a major factor governing the heat flux from the steel to the cooling water in the mould. The high conductivity of the mould wall material ensures a small temperature drop across the copper. The 'cold' face of the mould wall can be significantly higher than the bulk cooling water temperature due to the boundary layer which is present in any water cooling channel. This boundary layer, however, can be affected by the cooling water flow conditions in the cooling channel and the temperature drop across the boundary layer can be fairly confidently predicted from well proven heat transfer theory. It is

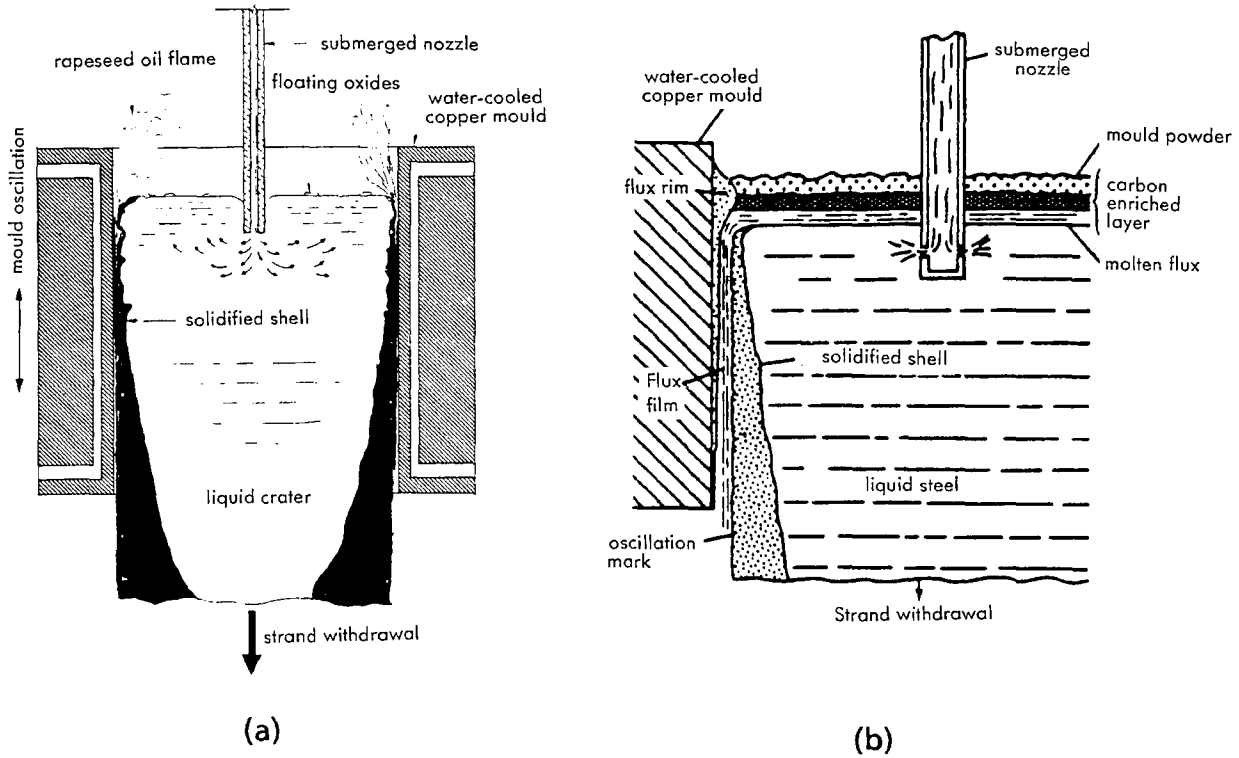


Figure 3.9 Teeming and mould details for lubrication using (a) rape seed oil and (b) mould powder to provide a slag.

necessary to maintain the cooling water velocities sufficiently high (8 m/s) to avoid nucleate boiling.

The interface between steel and copper, the major component to the thermal impedance, is a complex area and needs discussing in more detail. This is very much affected by the type of lubricant used.

In billet casting squares <~130 mm and rounds <~130 mm diameter it is difficult to use a refractory submerged entry nozzle. In these cases 'open' teeming using a metering nozzle is practised but invariably using an inert gas shroud around the open teeming stream (see Figure 2.10). Rape seed oil, fed from small holes in the copper face above the meniscus, is used as a lubricant in this case. Figure 3.9 (a) shows the details in the mould when using rape seed oil as the lubricant.

In slab and bloom casting a submerged entry nozzle (SEN) is used together with a synthetic mould powder which forms a fluid slag between the powder and the steel in the mould. Figure 3.9(b) shows the details in the mould and the interface with the copper when using a submerged entry nozzle and synthetic powder.

The main advantages of using mould powder over rape seed oil are:

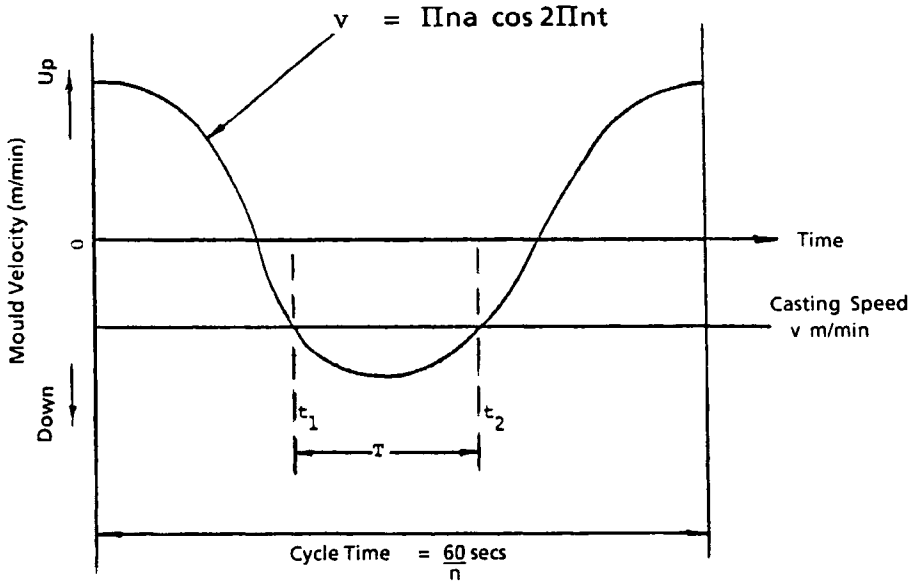
- A submerged entry nozzle (SEN) is used with mould powder which is a more efficient method of stream shrouding.
- It prevents radiative heat losses from the metal surface in the mould and prevents solidification on the surface which can lead to 'plating' defects.
- The slag formed from the powder absorbs non-metallic inclusions (e.g.  $\text{Al}_2\text{O}_3$ ) which float out of the metal pool in the mould.
- The slag allows more uniform heat transfer to the copper wall.

The mould powder composition and properties needs to be such that the heat from the liquid steel produces a continuous fluid slag layer of adequate thickness and with a viscosity which enables a continuous flow of slag into the meniscus at the copper wall.

A further fundamental requirement is that the mould is oscillated sinusoidally in such a manner that for a certain percentage of the cycle the mould would be travelling in a downward direction faster than the solidifying shell.

Figure 3.10 shows the oscillation cycle and that part of the cycle where the mould travels downwards faster than the strand. This is called the negative strip time, or heal time, and is chosen as a compromise between lubrication (and hence friction) and the maintenance of uniform heat transfer. This will be discussed in much more detail in Section 4.2.3.3.

The interactions between the mould oscillation, mould slag feeding and variations in mould metal levels are quite complex and several computer



$T$  = Heat Time (secs)

$a$  = Stroke Length (mm)

Figure 3.10 Oscillation cycle showing negative strip time.<sup>1</sup>

models have been developed<sup>8</sup> to determine the mould powder consumption rate and the solidification characteristics at the meniscus as a function of mould oscillation, mould level and powder slag properties. This will be discussed further in Section 4.2.3.2.

All these factors determine the slag film thickness which in turn determines the thermal impedance of the interface. Additionally, the gap between the solidifying steel and the copper wall is affected by the surface temperature and shell contraction, which can cause 'air' gaps to form which may depend on section size and shape. Figure 3.11 shows for various strand cross-sections the formation of an 'air' gap between the strand shell and the mould wall such as occurs below the meniscus level.

These gaps can also vary down the length of the mould usually increasing from below meniscus level. This is counteracted by a three-dimensional taper for billet and bloom cross-sections. In the case of slab moulds only the narrow faces follow the shrinkage in the cross-section and only the end plates are consequently tapered. Due to bulging no gaps form along the broad faces for slabs and the broad faces are set parallel to each other.

Much work has been carried out<sup>7</sup> using thermocouples embedded in the mould copper plates to measure the heat flux through the mould

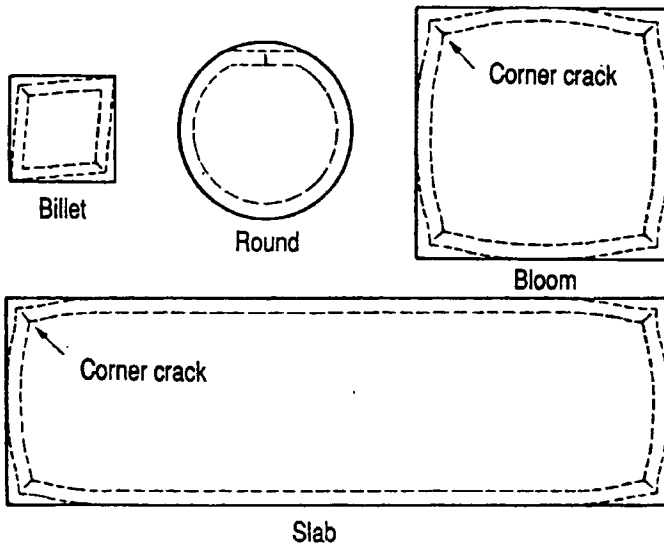


Figure 3.11 Gap formation and change in cross-section resulting from shrinkage in the mould.<sup>6</sup>

plates. This work has generally concentrated on the inter-relation of the heat flux, heat flux distribution, mould wall temperatures, type of mould lubricants used, steel compositional factors and operating practice. The implications of some of these factors on as-cast steel quality will be discussed in Chapter 4.

The general temperature distribution from the solidifying steel to the cooling water is shown in Figure 3.8. Figure 3.12 shows the location of thermocouples inserted in the copper end plate of a 330 mm × 254 mm bloom mould.

Thermocouples were arranged in pairs mid way between the water cooling channels. The thermocouples in each of these pairs were situated 7 mm and 18 mm respectively from the 'hot' face of the copper mould. 7 pairs were installed down the length of the mould as shown in Figure 3.12. This thermocouple arrangement enabled heat fluxes to be measured and the 'hot' face temperature of the copper plate to be calculated.

Both mould wall temperatures and heat flux distributions down the length of the mould were investigated. These investigations included the effect of:

1. The flow-rate and hence the velocities of the cooling water.
2. Type of mould lubricant used.
3. Carbon content of the steel being cast.
4. Casting speed

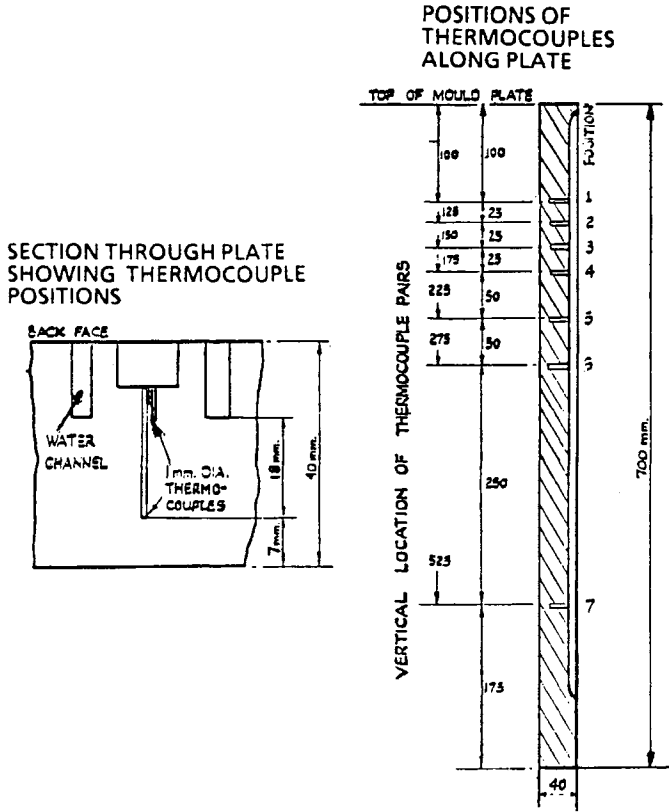


Figure 3.12 Location of thermocouples in a 254 mm end plate.

### 3.1.2.1 Effect of Cooling Water flow-rate

The cooling water flow-rate was varied over a wide range and Figure 3.13 shows the effect of the cooling water flow-rate on heat flux and 'hot' face copper temperature.

It can be seen that the heat flux is fairly constant for this wide variation in the cooling water flow-rate which confirms the point made that the over-riding controlling factor on heat extraction from the solidifying steel is the interface boundary between the steel and the hot face of the copper mould. The effect of the boundary layer can be seen to have driven the copper temperatures higher for a lower water flow rate.

### 3.1.2.2 Affect of Mould Lubricants

Figure 3.14 shows the effect of various mould lubricants on the heat flux distribution down the mould and on 'hot' face copper temperatures. These distributions are shown for two mould casting powders and for rape seed

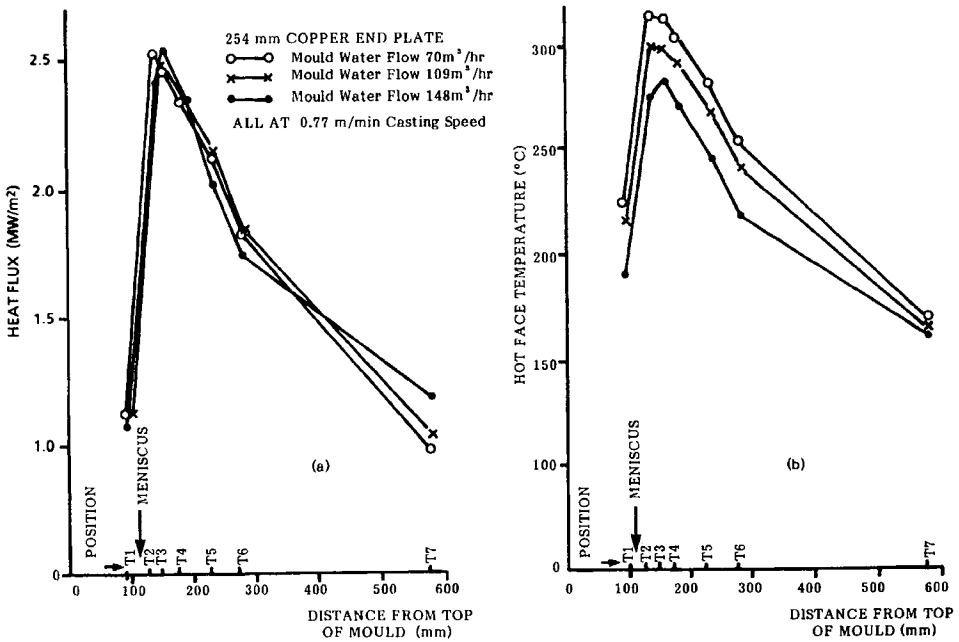


Figure 3.13 Effect of cooling water flowrate on (a) heat flux and (b) hot face temperature.

oil. As can be seen from these results, the heat fluxes are considerably higher for rape seed oil and it is worth noting in particular the very increased heat flux in the meniscus region.

### 3.1.2.3 Effect of Carbon Content

The effect of steel composition and particularly carbon content on the overall mould heat transfer has been reported from several sources.<sup>7,9</sup> Figure 3.15 shows the measured average heat flux in the mould over the carbon range of 0.02% to 1.6%. The effect of carbon content on heat transfer leads to some quality problems being more acute within the carbon range 0.06 to 0.14% (the peritectic range).

Irregular shell thicknesses down the length of the mould have been observed<sup>10,11</sup> for 0.1% carbon steels. It was proposed that this irregularity in shell thickness and in non-uniform heat transfer is caused by the  $\gamma$  to  $\delta$  phase transformation and associated volume changes and shrinkages which occur at this particular carbon level. Figure 3.16 shows the temperatures as measured by a thermocouple near the front face for two levels of carbon and, as can be seen from these recordings, the temperature fluctuations are lower at the higher carbon level (0.55%) while marked fluctuations occur during casting steel with 0.15% carbon. The lower heat fluxes

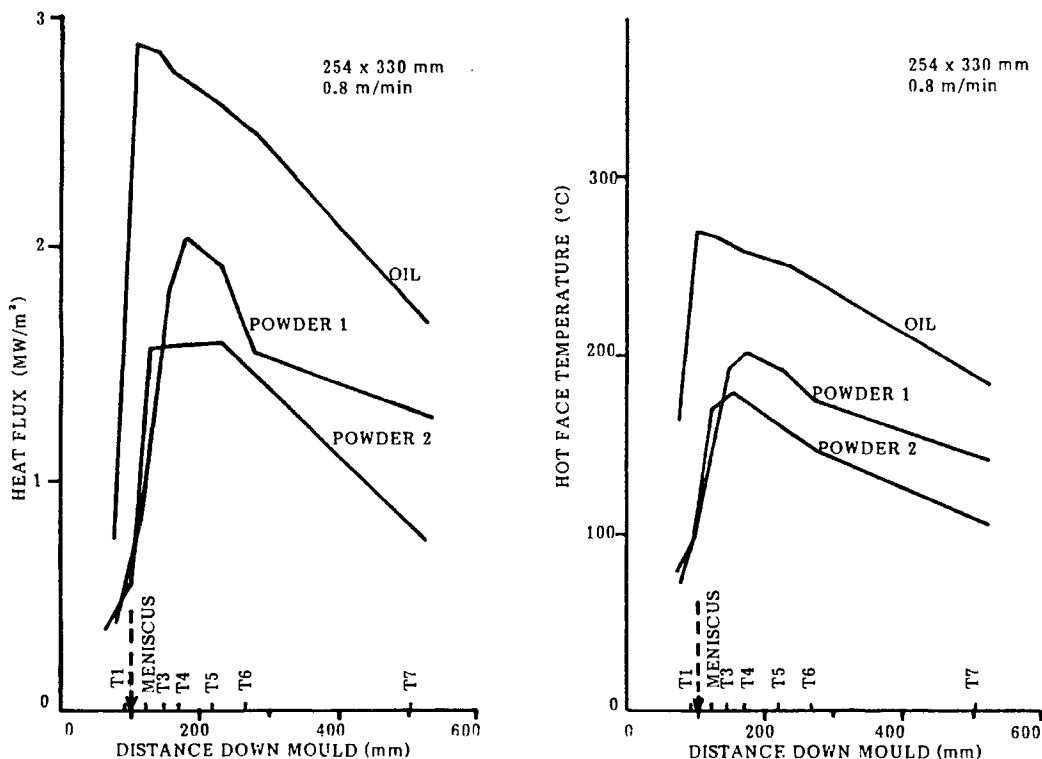


Figure 3.14 Affect of lubricant type on (a) heat fluxes and (b) hot face temperature.

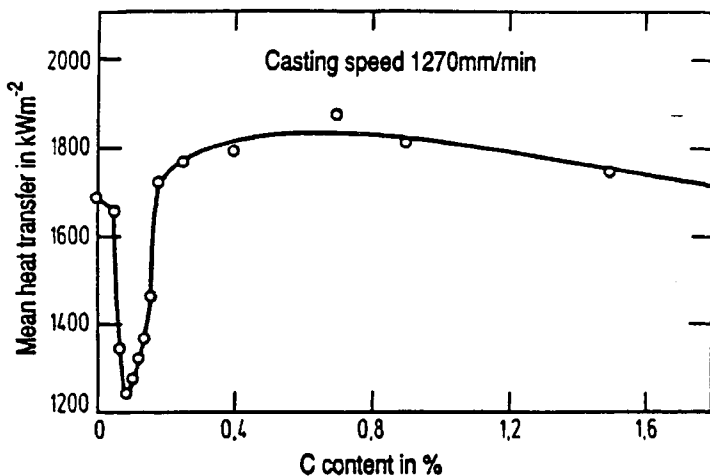


Figure 3.15 Affect of carbon content on mould heat flux.<sup>9</sup>

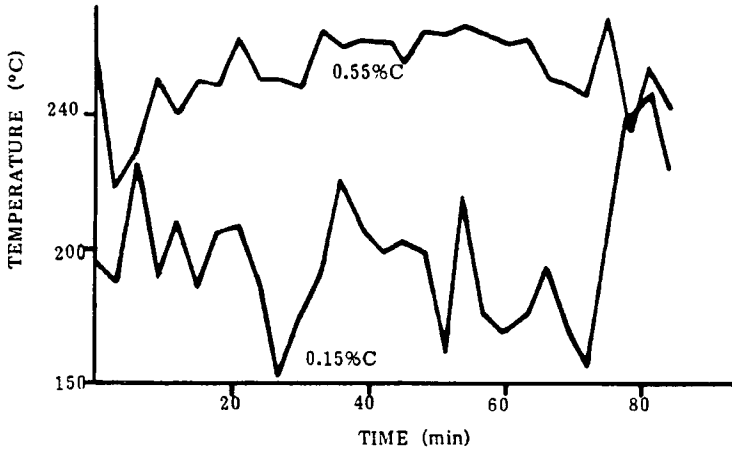


Figure 3.16 Thermocouple temperature for 0.55% and 0.15% C.

at around 0.1% carbon level lead to specific defects arising at these carbon levels and these will be discussed further in Section 4.2.2.1.

3.1.2.4 Effect of Casting Speed

Casting speed also has a marked effect on the distribution and mean heat flux in the mould. Figure 3.17 shows the mean heat flux as a function of the distance down the mould at different casting speeds ranging from 0.8 m/min to 1.3 m/min.

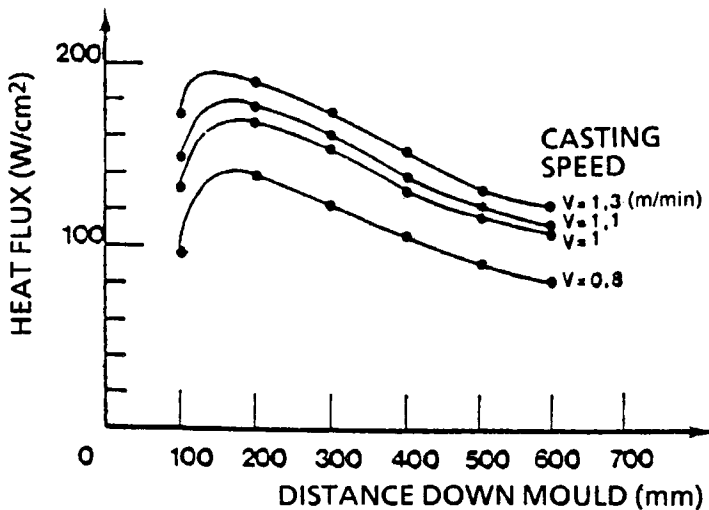


Figure 3.17 Heat flux down the length of the mould for various casting speeds.<sup>1</sup>

### 3.1.2.5 Copper Temperature Distribution

A computer model, which has been calibrated with the above experimental data, enables the complete temperature field within the mould walls to be calculated. <sup>7</sup> Figure 3.18 shows the vertical temperature field in the mould wall material along with measured data. The data which have been acquired by these many extensive plant measurements are used as the boundary conditions in the mould when running the strand solidification and temperature distribution mathematical model which is described in Section 3.4.1.

### 3.1.2.6 Heat Transfer Measurements on a Slab Mould

A more comprehensive number of thermocouples were inserted into a slab mould copper plate and Figure 3.19 shows the arrangements for these thermocouple pairs.

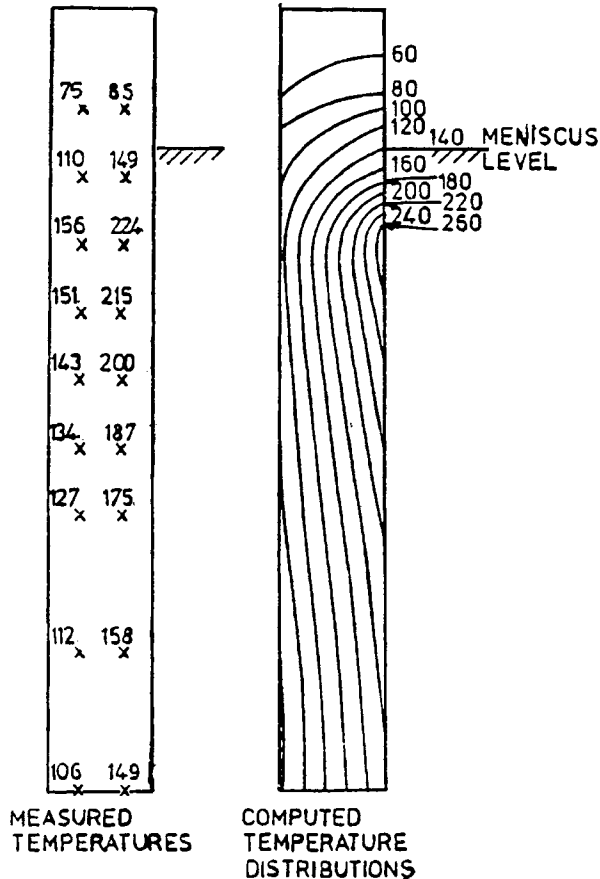


Figure 3.18 Computed and measured temperatures in the vertical section of the 254 mm copper end plate.

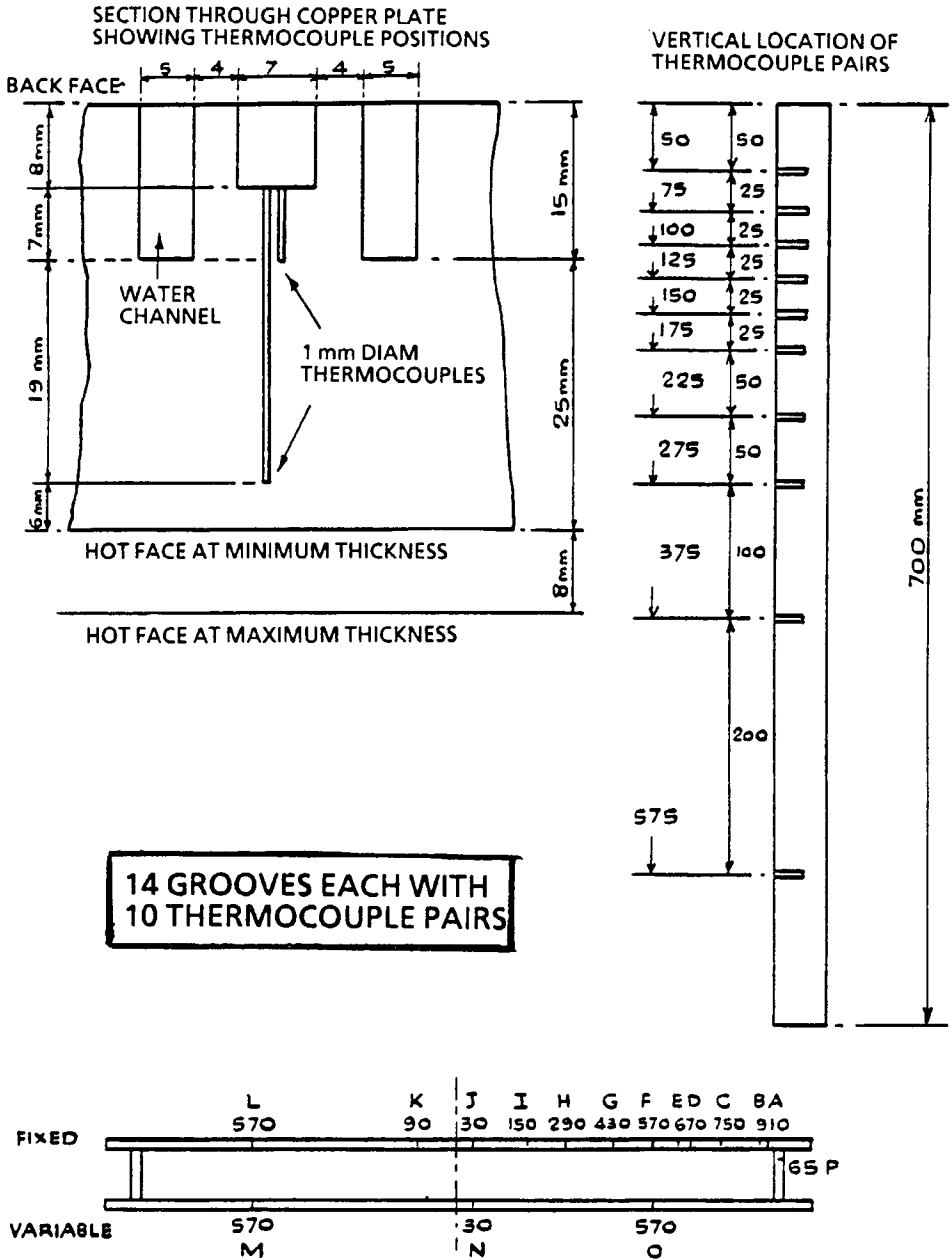


Figure 3.19 Arrangement of thermocouple pairs in a slab mould broad face copper plate.

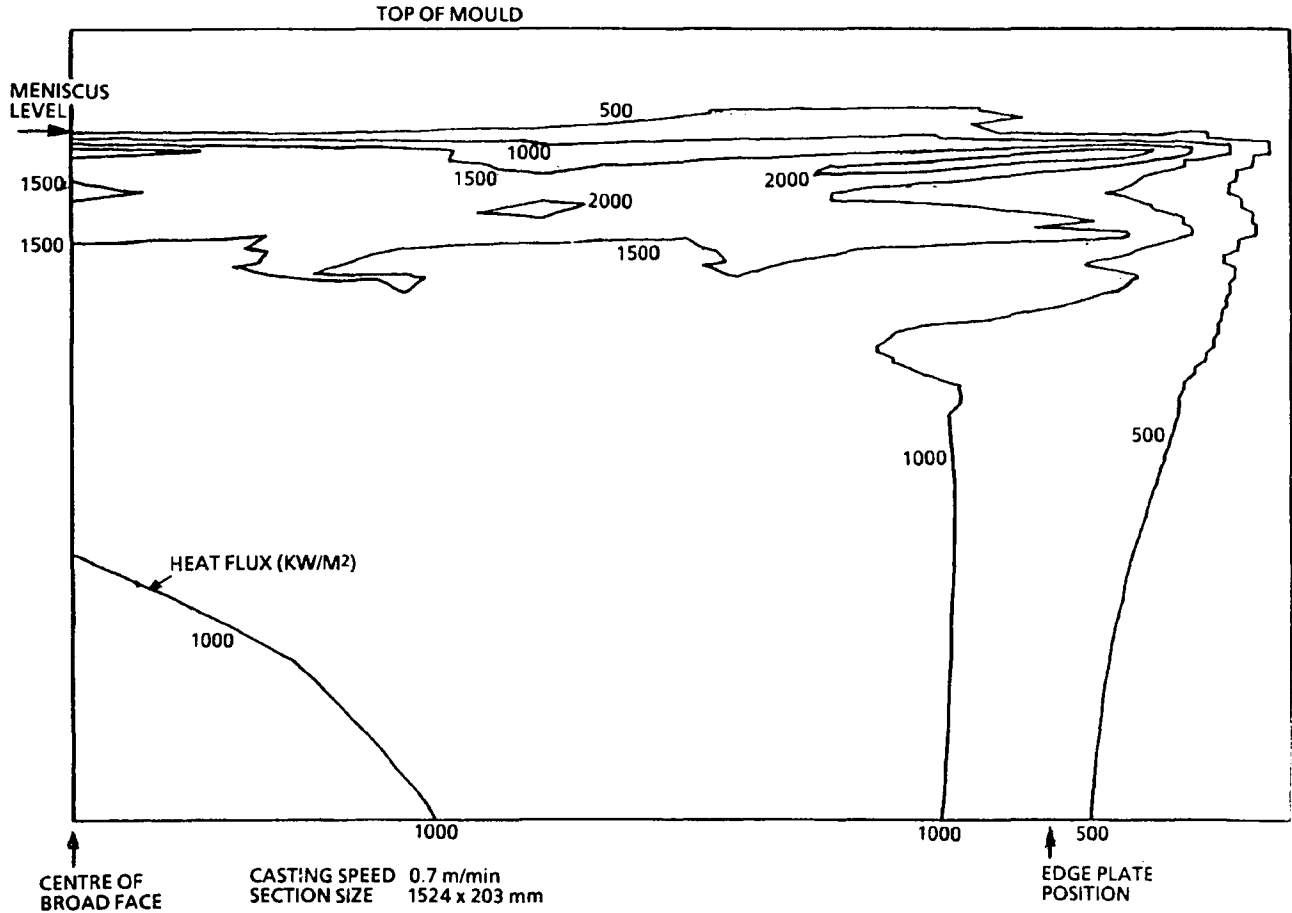


Figure 3.20 Heat flux contours for one half of a slab caster broad face copper plate.

The heat flux contours of one half of the broad face copper plate are shown plotted in Figure 3.20.

## **3.2 Strand Support Systems and Secondary Cooling**

The partly solidified shell as it emerges from the mould is in the region of 10–25 mm thick (depending on casting speed) with a surface temperature of around 1000°C increasing to the solidus temperature (~1500°C) at the solid/liquid interface. It is subject to the ferrostatic pressure of the liquid steel and would consequently quickly bulge outwards without constraint.

This thin shell, as it emerges from the mould, requires both continual cooling and mechanical support. Secondary cooling sprays are used to control the cooling but the strand support structure, being water-cooled for protection, also extracts heat from the strand. Radiation also contributes to the total heat transfer. The design and operation of the secondary cooling system is dependent on the type and design of the strand support system which in turn depends on the section size and shape being cast. The details of the support equipment for various machines will first be described.

### **3.2.1 Strand Support Systems for Various Machine Types**

The strand support systems vary considerably between those required for billet, bloom and slab casters. For small square sections such as billets the restraining influence of the billet corners are sufficient to prevent shell bulging apart from the region just below the mould. In this case the mould foot rollers combined with support rollers on each side for the first metre or so may be adequate support. This gives more scope further down the strand for more uniform cooling from sprays. However, some billet casters, operating at lower casting speeds and producing section sizes less than about ~130 mm square or rounds with diameters less than ~150 mm have no containment support other than the foot rolls attached to the mould. Any rolls in such machines are usually just to guide the strand and to re-thread the dummy bar. For higher casting speeds for billet casting more support rollers may be required. In any such event the alignment of these rolls with each other and the mould exit is quite important.

The mould length is usually between 700 and 900 mm long (see Section 3.1) but for some billet machines casting at higher speeds a mould extension device is sometimes used. This consists of four spring loaded plates with cooling being provided through orifices in the plates. This mould together with the extension is termed the 'Multi Stage (MS) Mould'.

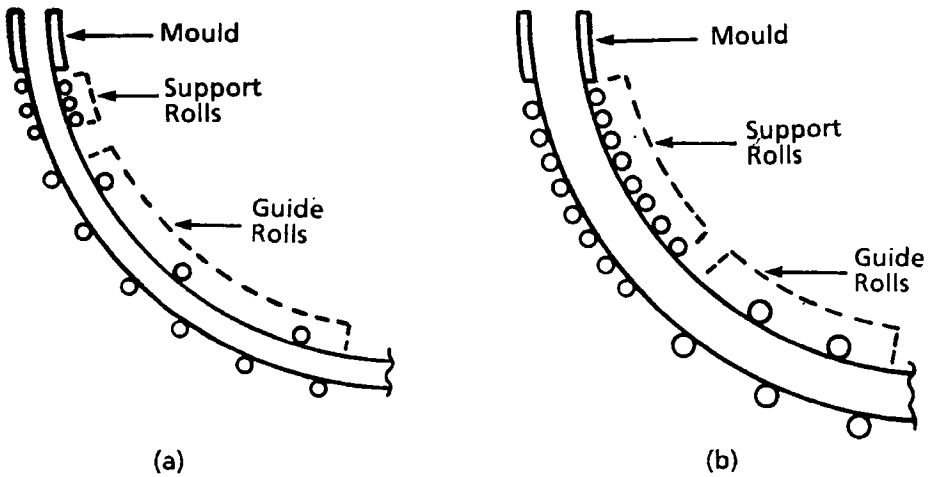


Figure 3.21 Extent of support rollers for typical billet and bloom casters.

For larger billet casters and bloom casting there is an increased propensity for bulging when the shell is still hot and thin and consequently support rolls have to extend further down the strand. Typical support systems for a billet machine and a bloom machine are given in Figure 3.21.

For slab machines the bulging of the broad faces extend to the point where solidification is complete and invariably strand support of the wide faces extends the full length of the machines. The latter part of the machine requires rollers for strand withdrawal. Since slab machines are the most complex by both the extent of the support, and the bulging forces involved, the detailed description of the design and operation of strand support systems will concentrate on slab machine requirements. It should be noted that the strand support system contributes significantly to the cooling of the strand and these cooling affects will be included in Section 3.2.2. on 'Secondary Cooling'.

### 3.2.1.1 Below Mould Support for Slab Casters

A variety of strand support and cooling systems just below the moulds in slab machines have or are currently being used. These are:

- Rollers
- Grids
- Cooling plates
- Walking beams

Walking beams proved to be mechanically too complex whilst cooling plates generated too much friction.

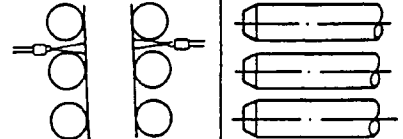
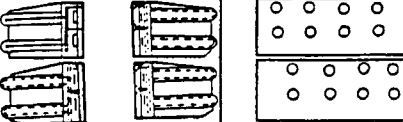
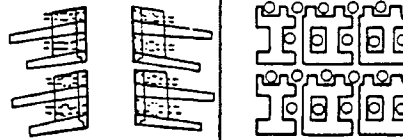
	Schematic diagram			Secondary cooling water covering ratio	Slab supporting ratio	Withdrawal resistance	Remarks
Roll		13.7%	3.0%	Low	Direct cooling system (flat spray)		
Cooling plate		3.7%	89.3%	High	Indirect cooling and direct cooling system		
Cooling grid		25.6%	56.3%	Medium	Direct cooling system (full cone spray)		

Figure 3.22 Characteristics of below mould support systems for slab casters.<sup>12</sup>

The aim is to obtain uniform cooling with minimum friction whilst maintaining accurate support geometry. Today rollers and grids are in most common use with rollers providing the system with least friction between strand and support system.

Figure 3.22 gives details of the characteristics of rollers, cooling plates and grids.

The secondary cooling arrangement just below the mould very much depends on the strand support system used. For example, with rollers flat sprays are used because of the small gap between the rollers. For grids, however, full cone sprays are used and aligned to direct the cooling water into the rectangular apertures in the grid. With cooling plates the water is directed through a matrix of small holes and the resulting water film between the plate and the strand provides the cooling.

### 3.2.1.2 Main Strand Support Systems for Slab Machines

In a continuous slab caster the main support systems are generally composed of segments containing between three to six pairs of rolls with the ability to rapidly exchange the whole segment. The segment frames are clamped together by hydraulic cylinders and the roll gaps are preset using chocks and shims. Figure 3.23 shows the details of a typical slab machine segment (a) with single piece rolls, (b) with 'divided' or 'split' rolls and (c) the end view.

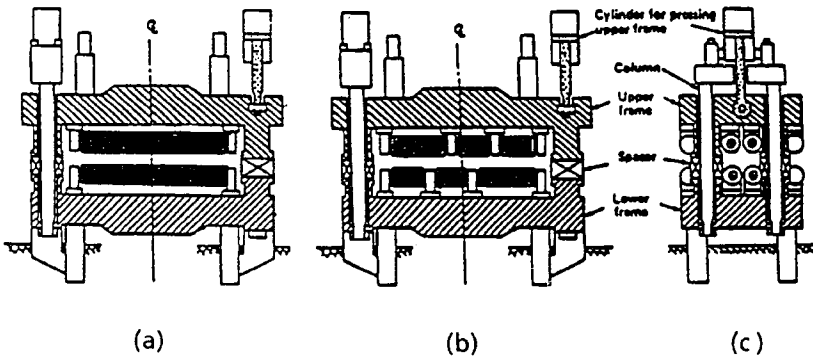


Figure 3.23 Details of typical roller support segments (a) with single piece rolls, (b) with divided rolls and (c) end view.

The secondary water sprays are aligned on headers so that the solidifying strand is cooled in the gaps between the rolls.

The segment as a whole is fixed rigidly to the frame of the casting machine and the inner radius rolls can be adjusted by the hydraulic cylinders to enable a change of casting thickness (by selection of thicker chocks) or for fully opening which is required in the case of an over cooled slab in the machine which has to be removed by cutting or for scheduled maintenance of the segments *in situ*.

It is necessary to have the facility to rapidly exchange the segments and Figure 3.24 shows a schematic diagram of how each segment can be withdrawn from the machine by way of guide rails along which a crane lifts the segments from the machine.<sup>12</sup> In some machines the segments are removed horizontally sideways prior to lifting them out by use of a special crane.

Complex finite element models have been developed to predict the degree of bulging of the solidifying shell both between adjacent roll contacts and when a roll is misaligned with respect to the adjacent rolls. These will be described in para 3.4.2. Such models are used to design the optimum diameter and pitch of the support rolls. The pitch has to be such that there is insignificant bulging between the roller contacts and the rolls need to be of such a diameter that minimises the degree of roll bending due to the ferrostatic force generated by the liquid core and the thermal stresses due to non symmetrical heating of the rolls.

Up to about 1980 most slab machines used single piece rolls but over the last decade there has been a significant increase in the application of 'divided' or 'split' rolls. Single piece rolls extend to over the full width of the strand and are supported by bearings at each end of the roll (see Figure 3.23). With the advent of improved bearing technology (cooling

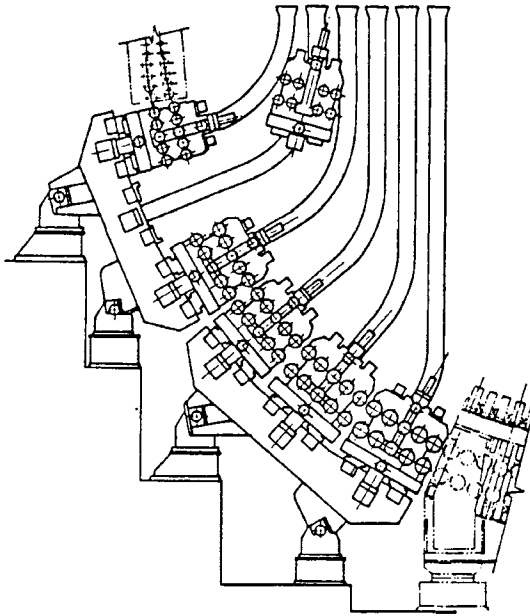


Figure 3.24 Removal of segments via vertical guide rails.

and lubrication in a hot environment) most new wide slab casters and many which have been rebuilt now contain divided rollers. Divided rollers consist of shorter lengths of roller barrels supported part way across the strand by 'central' bearings. This allows greater scope to reduce roll diameters and pitches whilst maintaining rigidity and hence roll gap geometry.

The effect of roller design and performance on slab quality will be discussed fully in Section 4.2.5 (surface quality) and Section 4.3.5 (internal quality). Much work has been done to evaluate the performance of various roller designs and details of their behaviour as a function of design and other operating parameters are more fully discussed in Section 3.2.3. Details of mathematical models to support this work are described in Section 3.4.3

### 3.2.2 Secondary Cooling

The total 'secondary cooling' is a combination of several components which are:

- Cooling due to radiation
- Cooling due to the water sprays both by the evaporation of the spray water droplets on the slab surface and by the deflected water which accumulates in the entry nip between the rolls.

- Cooling by conduction to the rolls (see para 3.2.3).

In this section details will concentrate on the water sprays themselves but the design and operation of these sprays are very much dictated by the strand support design and as such the individual effects of the sprays on strand solidification cannot always readily be separated.

As described earlier high intensity water sprays are used between the support rollers to further accelerate the solidification process and to assist in controlling of, and reducing fluctuations in, the strand surface temperatures.

The secondary spray cooling achieves the following:

- The main purpose is to extract heat from the solidifying strand.
- The spray nozzles can be designed, arranged and the water flow-rates controlled to give an optimum surface temperature which is necessary to achieve the required surface quality.
- The spray water contributes to the cooling of the strand support rollers although these are all internally cooled (see Section 3.2.3).

In the earlier days of continuous casting of steel water only nozzles were used for secondary cooling but during the late 1970s and early 1980s air-mist sprays were introduced on a wide scale. These consist of both a water and air supply to a nozzle at high pressure resulting in a much finer water particle size whilst also having a wide angle. This enables a much more uniform application of water and the smaller particle size has the advantage of increasing the heat transfer coefficients. Figure 3.25 shows the two systems.

To obtain the basic heat transfer coefficients for both water and air-mist sprays much work has been done in various laboratories. The water flux

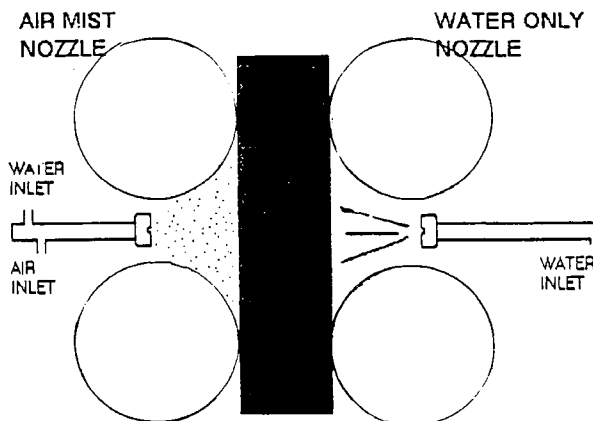


Figure 3.25 Arrangement of water only and air mist spray systems.

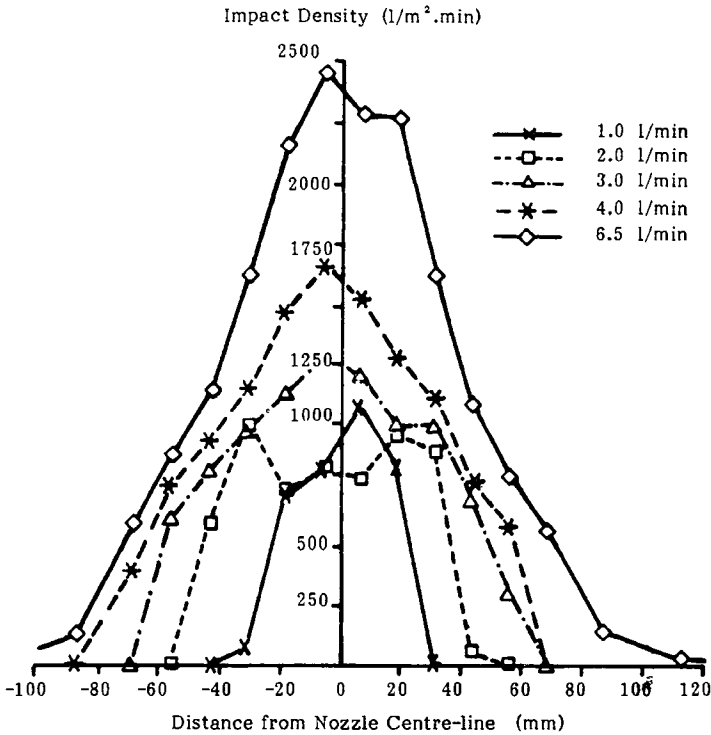


Figure 3.26 Transverse impact density distribution.

distributions and the heat transfer distributions have also been acquired during such measurements. Figure 3.26 shows the transverse impact density distributions for various flow-rates for a particular nozzle. The impact density is defined as the flow-rate per unit area ( $L/m^2 \cdot min$ ).

Figure 3.27 presents a correlation of heat transfer of water spray cooling data after the subtraction of the radiation component. The correlation is based upon the measured data from a number of studies.<sup>13, 14, 15, 16</sup>

The data have been rationalised into two equations, these being:

$$q = 16 V_s^{0.75} \text{ W cm}^2 \text{ (at 2.5 bar)}$$

and 
$$q = 22 V_s^{0.75} \text{ W cm}^2 \text{ (at 8.4 bar)}$$

where  $q$  = heat flux ( $W/cm^2$ )

$V_s$  = Water impact density ( $L/m^2 \cdot s$ )

The difference of 38% for the heat flux at these two pressures is attributed to the discharge velocity.<sup>13</sup>

The heat transfer arrangements and required surface temperature profiles are different for machines casting billets, blooms or slabs but in each

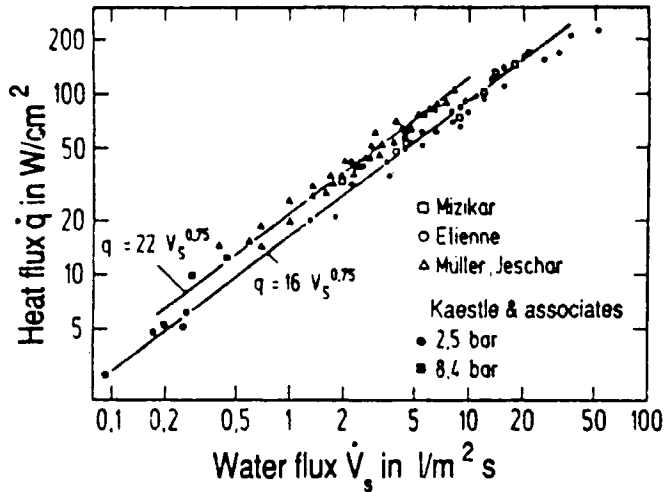


Figure 3.27 Correlation of heat transfer of water sprays after the elimination of the radiative component.

case the cooling is controlled to optimise surface quality. The criteria for the surface temperature profiles invariably depends on the high temperature properties of steel (see Section 4.2.2.2.) and are influenced to some extent by internal quality requirements. There are, however, many fundamental similarities in the secondary cooling of all section sizes and the same theoretical and practical principles can be applied.

The water spray pattern impinging on the strand surface should cover as wide an area as possible but this is often made difficult by the presence of the strand support system. Full cone nozzles are able to cover a large round or square impact area whilst flat spray nozzles can cover a wide impact area across the strand but only a small distance in the direction of casting when used to direct water between adjacent rolls. In billet casters, full cone nozzles are predominately used mounted on header pipes which are installed vertically along each face of the billet strand. The location of support rolls in the upper part of bloom casters and for the whole length of slab casters invariably means that flat spray nozzles have to be used. The length of the entire spray section varies between 0.5 and 6.0 m in the case of billet and small bloom casters and can extend up to 20 metres in high speed slab casters. The secondary cooling system is divided into a number of independently controllable zones down the length of the machines. The spray water supply systems are quite independent of both the mould cooling water and the 'closed' water system to cool the rolls and bearings and other machine elements.

Where air mist cooling is employed, atomisation is by high pressure compressed air acting as the carrier gas. The steam generated is extracted from the spray chamber by large fans. The non vaporised water which may contain scale and grease is returned down a flume beneath the caster to the water cooling and cleaning plant.

### 3.2.2.1 Spray Cooling with Water Only

In secondary cooling with water alone, the atomisation of the water occurs at the nozzle by virtue of the water supply alone, without additional assistance from other media. In slab casters, the number of horizontal trajectory nozzles located between the rolls determines the system nomenclature. A single-nozzle system denotes the arrangement of one nozzle (occasionally two) which produces a wide-angle spray (up to  $120^\circ$ ) at each inter-roll space (spray zone); the multi-nozzle system involves the grouping of many nozzles with a small spray angle at each spray zone. Figure 3.28 shows these alternate nozzle system arrangements.

The single-nozzle system is currently well suited to the majority of the usual slab grades and sizes produced. It began to replace the multi-nozzle system around the mid 1960s because the small nozzle orifices of the latter tended to become clogged very easily. In the meantime, the multi-nozzle system has been revived for certain casters for sheet and sensitive grades, with high spray water flux in conjunction with high casting speeds. The water employed in such systems must have only a minimal content of suspended particles.

The advantages of the single-nozzle system are obvious: fewer nozzles, simpler supply system and easier to maintain. As the single nozzle is installed further away from the strand, it is better protected. Another important benefit in wide-angle single nozzles lies in their relatively high flow capacity (same volume of water with fewer nozzles = greater throughput

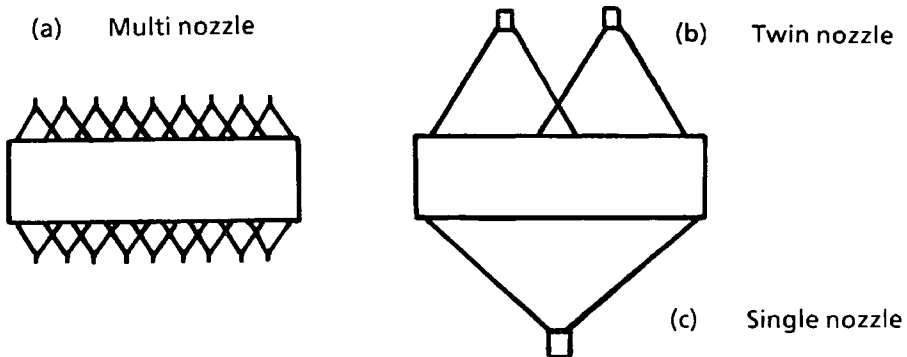


Figure 3.28 Alternative nozzle system arrangements.

per nozzle) and hence a larger outlet bore. The outlet bore determines the capacity range of a nozzle, and the flow-rate is controlled within this range by the water pressure. However, large changes in pressure also alter the spray angle, and if the pressure becomes too low, the spray angle collapses and the water flows out of the nozzle orifice without the desired spray effect. The lower pressure limit is generally considered to be 0.5–1.0 bar.

A disadvantage common to all spray nozzles in water-only systems is their comparatively narrow volume flow control range which, given the usual operating pressure encountered in continuous casting plant of 1.0–8.0 bar (at the nozzle tip), is only 1 : 3.5 on average.

In continuous casters in which slabs of various steel grades have to be cast over a very wide range of casting speeds, this limited control range of the nozzles in water only cooling systems may render the installation of two separate spray systems necessary in order to produce the necessary range in water flux. Such systems feature two nozzles of different ratings arranged side-by-side at each cooling zone, and depending on the required water flux, either the smaller, the larger or both nozzles together are employed. Dual systems of this kind are, of course, more expensive and complex.

### *3.2.2.2 Spray Cooling with Water and Air (Air Mist)*

In water-air mist spray cooling systems, the cooling water is mixed with compressed air in a mixing chamber ahead of the nozzle, and the mixture emerges from the nozzle as a finely atomised, high-impulse, wide-angled spray. This type of spray cooling is particularly suitable for high-grade steels which are susceptible to cracking. Its more important advantages include a particularly uniform cooling pattern and a very wide volume flow control range.

A combined air and water cooling system can easily offer a volume flow control range of 1 : 12 and more. The most important benefits of this system are:

- Large flow-rates from nozzle orifices, therefore little danger of nozzle clogging.
- Large volume flow control range, therefore only one nozzle type required for all steel grades and casting speeds
- Uniform water flux over a wide slab surface area (from roll line to roll line), therefore reduced danger of local over-cooling of the strand surface for a given overall rate of heat extraction.
- Formation of extremely fine water droplets for optimum cooling effect.
- Efficient vaporisation of the fine droplets results in less water accumulation ahead of the roll nip.

### 3.2.3 Roller Design and Performance

The design of the support rollers in continuous casting machines for slab production is a compromise of several factors. As indicated in Section 3.2.1.2 for slab casting machines installed before 1980 the majority of the support rollers were a single roll with support bearing at each end. In the early 1980s with the advent of the development of bearing technology to resist the adverse environmental conditions in the machine, two or three piece rollers were used. Figure 3.29 shows the change in roller pitches for new machines supplied prior to and after around 1980.

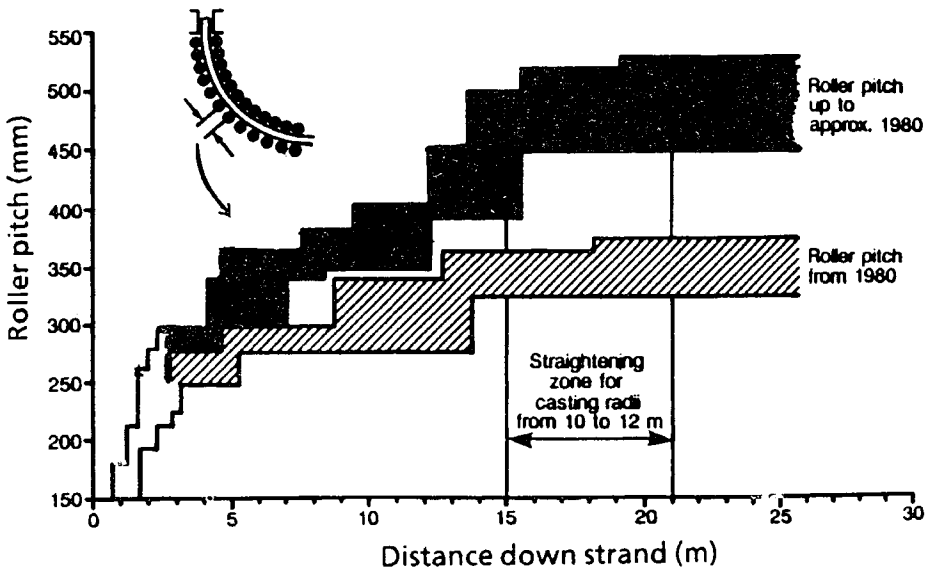


Figure 3.29 Comparison of roller pitches prior to and after 1980 for new slab machines.

All rollers and bearings need to be water cooled and apart from some of the smaller rolls in the upper part of the machines (where high secondary water flow-rates are used) all rollers are internally cooled. However, there are several different designs of rollers and the internal cooling efficiency can vary from one design to another. The main requirements of support rolls are:

1. The diameters and pitches should be such that the inter-roll bulging of the strand should be minimised. This in turn depends on the degree of secondary cooling (i.e. the strand temperature), the casting speed (primarily determines shell thickness), the distance down the strand, and the grade of steel. The creep properties of steel can vary significantly

depending on steel grade. On a 12 m radius machine the ferrostatic pressure at the tangent point is 86 t/m<sup>2</sup> so the force on the solidifying skin is quite large. The degree of bulging is also time dependent and therefore the time taken for a particular element of the solidifying shell to pass from one roll to the next is related to casting speed.

2. Geometrically the rolls should remain stable. If the rolls were too small in diameter and maybe 2 metres long (a typical slab single roll length) then the rolls would bend due to:
  - (a) the ferrostatic force
  - (b) the thermal stresses since the rolls have an asymmetrical temperature distribution during operation.
  - (c) during a strand stoppage the asymmetric temperature is magnified considerably.

The water cooled support rolls themselves can extract a significant amount of heat from the solidifying strand and the amount of heat extracted depends on the roll design. The various types of roll designs and roll cooling methods are illustrated in Figure 3.30 which shows the main roll design and cooling methods.<sup>17</sup> Examples are for single piece rolls but many of the principles also apply to divided rolls.

Because the cooling channels of the peripheral-bore design and the scrolled design are near the surface the roll surface is kept colder.

These are commonly called 'cold' roll designs whilst the centrally bored cooling is termed a 'hot' roll design. The 'cold' roll designs extract significantly more heat from the strand than does the 'hot' roll design. However, the cold roll designs are more stable and much less prone to permanent bending when the strand stops and the roll bends due to grossly asymmetric temperature distribution leading to severe thermal stresses. If a roll

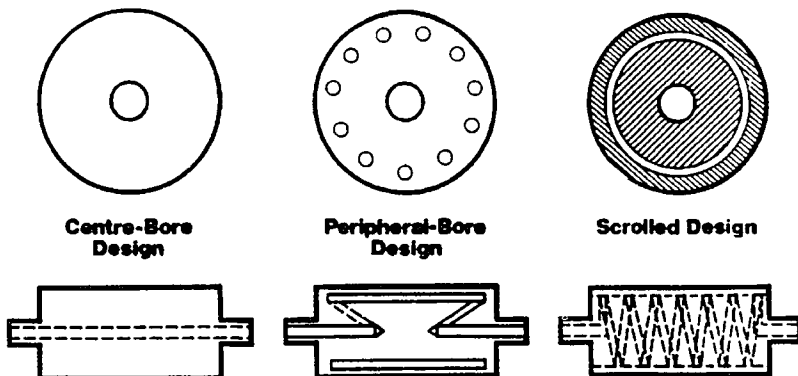


Figure 3.30 The different types of internal roll cooling.

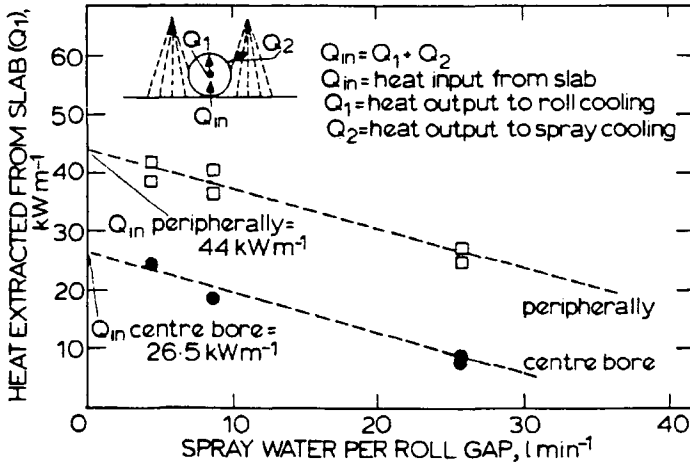


Figure 3.31 Heat extraction from the slab by the roll.

becomes permanently bent to a degree of greater than  $\sim 1$  mm at the centre this can lead to poor internal quality. The mechanisms of this poor quality are explained in Section 4.3.5

Much work has been done on evaluating roll performance both in terms of geometrical stability and heat extraction capability.<sup>18</sup> It is interesting to note that the amount of spray water used affects the heat extracted by the roll. Figure 3.31 shows the amount of heat extracted from both a peripheral bore roll and a centre bore roll for various amounts of spray cooling water entering the roll gap. With no spray water entering the roll gap the heat extraction is  $44 \text{ kW/m}$  and  $26.5 \text{ kW/m}$  respectively. (These values are the kW per metre length of roll).

Data have also been obtained on the geometrical stability of the various types of roll design.<sup>18</sup> Bulgemeters have been used to measure both roll behaviour and the bulging of the strand. These bulgemeters consisted of linear displacement transducers (LDT) on the end of units which were rigidly fixed in the machine with the LDTs resting on the back of the rolls or the strand surface as appropriate.

Three such bulgemeters at any single location in the strand are used, two on adjacent rolls and one on the strand between the two rolls. These instruments can be left in the strand over long periods and the behaviour of the rolls and strand have been investigated for many events such as strand stoppages or slow downs and for various secondary cooling conditions in casting different steel grades. Figure 3.32 shows such behaviour for 2 roll pairs at different positions down the strand both for a reduction in casting speed and when there has been a strand stoppage.

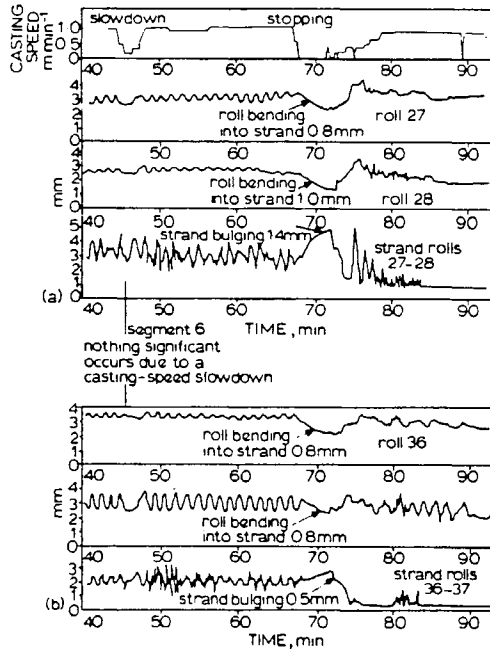


Figure 3.32 Roll bending and slab bulging during a slow down and strand stoppage at positions (a) 11 m and (b) 14.3 m from the meniscus.

Such deviations of roll geometry need to be avoided since these lead to unacceptable surface and internal quality. This is described in greater detail in Chapter 4.

All the work just described was carried out on single piece rolls which have to compromise between a sufficiently small diameter (and roll pitch) to prevent inter-roll bulging of the strand and a sufficiently large diameter to avoid bending under the mechanical and thermal loads to maintain good roll gap geometry. Over the last decade there has been a very significant increase in the application of split rolls as described previously (Figure 3.23). Most new wide slab casters and many which have been rebuilt now contain split rolls. This means that the individual roll barrel length is much reduced which reduces the bending of the roll significantly and thus allowing smaller diameters and roll pitches.

The roll gap geometry can also be affected by roll wear. The roll material is therefore also very important and a combination of roll material and efficient cooling can reduce roll wear as a serious cause of loss of roll gap geometry. The roll material needs also to be resistant to fire cracking and stress corrosion cracking and to meet these requirements the rolls are 'hard faced' with a layer of metal comprising 12 wt% Cr and 88 wt% Fe.

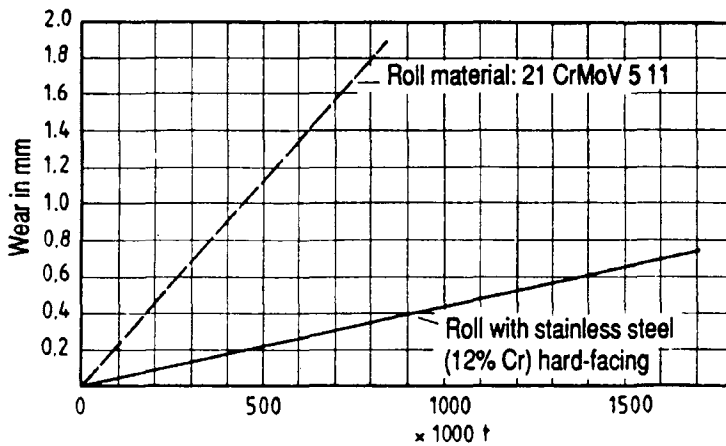


Figure 3.33 Roll wear as a function of material and tonnage produced.<sup>6</sup>

Figure 3.33 shows the effect of this surface on roll wear for 360 mm diameter rollers.

### 3.3 Strand Straightening and Strand Withdrawal

For casting machines, where the strand is either cast in a curved mould or is bent into a curved position below the mould, the strand requires to be straightened before it can be discharged horizontally. The design of the straightener (or the bending zone where the strand is curved after being cast in a vertical mould) is dependent on machine radius, section size, steel grades to be cast and other casting parameters. Details will be described in Section 3.3.1 below.

Additionally, sufficient power and traction need to be imparted to the strand to enable withdrawal to be reliable and consistent. Details are given in Section 3.3.2.

#### 3.3.1 Strand Straightening

As indicated previously, the curved strand needs to be straightened to achieve horizontal discharge. The design of the straightening unit depends on several factors and it is important to ensure that any stresses caused by the strains imposed due to straightening are smaller than the inherent strength of the material.

The strain distortion across the fully or partially solidified strand can be determined from standard beam bending theory but due to the tempera-

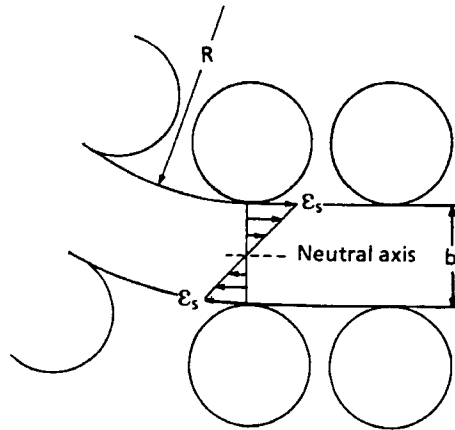


Figure 3.34 Strain distribution across the solidified strand during single point straightening.

tures involved creep occurs and hence to design for the overall strains required to straighten the strand the strain rate is also an important consideration. The strain distribution across the strand also depends on whether the strand is completely solid or whether a liquid core still exists. In modern machines requiring higher throughput a liquid core usually exists during straightening. The two situations will be dealt with separately.

### 3.3.1.1 Strand Completely Solidified

The strain distribution in this case depends entirely on the initial curvature and strand thickness and is shown in Figure 3.34.

The the surface strain is

$$\epsilon_s = \frac{b}{2R} \times 100\%$$

this being a tensile strain on the top surface and a compressive strain on the bottom surface. The strain rates can be reduced by applying the required strain over more than one unbending point or even continuously straightening over a given length of strand. These systems will be described later.

### 3.3.1.2 Straightening with a Liquid Core

In this case both the upper and lower solidified shell is considered as separate beams but the calculated strains can depend on the constraining influences of the solidified edges. These can be significant at low aspect ratios, when the solidified shell has reached a significant thickness and the shape of the shell has been influenced by the two dimensional heat

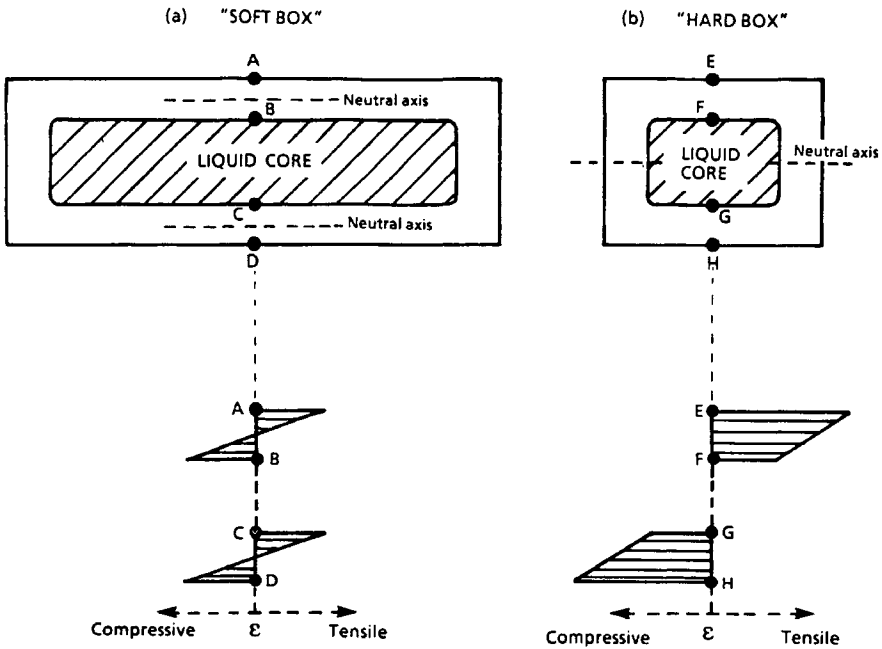


Figure 3.35 Strain distribution in solidifying shell using (a) the 'soft box' approach and (b) the 'hard' box approach.

transfer. Two approaches are therefore adopted. These are termed the 'Soft Box' and 'Hard Box' approach respectively(19).

- *'Soft Box' Approach.* The strand is considered to be a 'soft box' when the upper and lower solidified shells deform independently of each other i.e. there is no restraining influence of the solid edges. This is the situation in the case of a slab where the aspect ratio is high and the shell thickness small compared to the slab width. Figure 3.35 shows the strain distribution occurring in the solidifying shell due to straightening at the tangent point.

The neutral axis is assumed to be along the centreline of both the upper and lower shell although this is not strictly true because of the temperature gradient. It has been shown by using finite element analysis that the true neutral axis is nearer the cold surface.<sup>20</sup> There are tensile strains both at top outer surface and at the solid/liquid interface of the lower shell. These strains are a function of strand radius and shell thickness at the point of straightening.

The surface strains in this case are given by

$$\epsilon_s = \epsilon_i = \frac{t}{2R} \times 100\%$$

where  $\epsilon_s$  = outer surface strains; (tensile at A: compressive at D)  
 $\epsilon_i$  = solid/liquid interface strains (tensile at C: compressive at B)  
 $t$  = shell thickness (m)  
 $R$  = machine radius (m)

● *'Hard Box' Approach.* In this case the bending is primarily influenced by the stiffness of the solidified edges and the neutral axis in this case is assumed to be along the section mid thickness and the surface strains are similar to the situation where the strand is totally solid i.e.

$$\epsilon_s = \frac{b}{2R} \times 100\%$$

The solid/liquid interface strains in this case are given by

$$\epsilon_i = \frac{b - 2t}{2R} \times 100\%$$

It has been demonstrated<sup>20</sup> that the 'soft box' approach is appropriate for slabs or large blooms with a high aspect ratio. The 'hard box' approach is only applicable to billet and small bloom sections.

As indicated earlier the strain rate often determines whether a crack defect (either internal or on the surface) will occur. The inherent strength of the steel particularly at the solid/liquid interface is very low at the temperatures involved (see Figure 4.3) but at these temperatures creep rapidly reduces stresses resulting from the strains imposed. Therefore by reducing the strain rate the stresses can be maintained at low values and total high strains can be achieved by spreading the straightening over a length of the machine. This is done by the use of multi point straightening.

Figure 3.36 shows such a design using 3 point straightening

At point A the radius changes from  $R_1$  to  $R_2$  and then at point B to  $R_3$ . Finally at point C an infinite radius is achieved so that the strand can emerge horizontally. Figure 3.37 compares the strains and strain rates for this case and that when the same initial radius strand is straightened at a single point.

In the limit continuous straightening<sup>(20)</sup> is used on some machines over a length  $L$  of the machine. In this case the strain rate is given as:

$$\dot{\epsilon}_s = \frac{(\epsilon_s)v}{L} \text{ per min}$$

where  $v$  = casting speed in m/min  
 $L$  = length of continuous straightening unit (m)

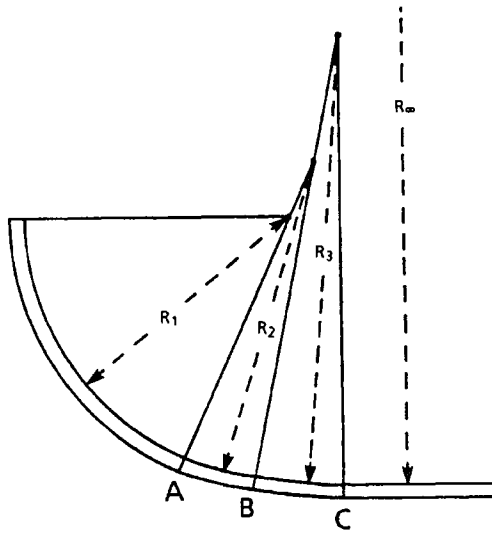


Figure 3.36 Strand showing three-point straightening.

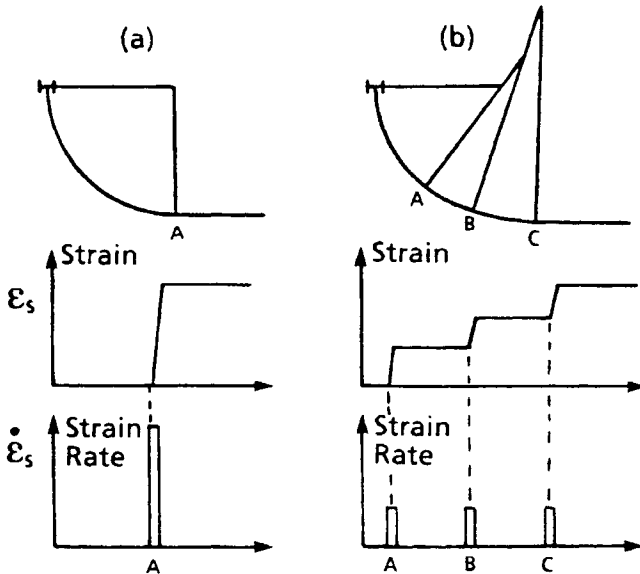


Figure 3.37 Surface strains ( $\epsilon_s$ ) and strain rates ( $\dot{\epsilon}_s$ ) for (a) single and (b) multi-point straightening.

### 3.3.2 Strand Bending

In the situation where a vertical straight mould is used the strand is bent to the appropriate radius below the mould. In this case the solidified shell is

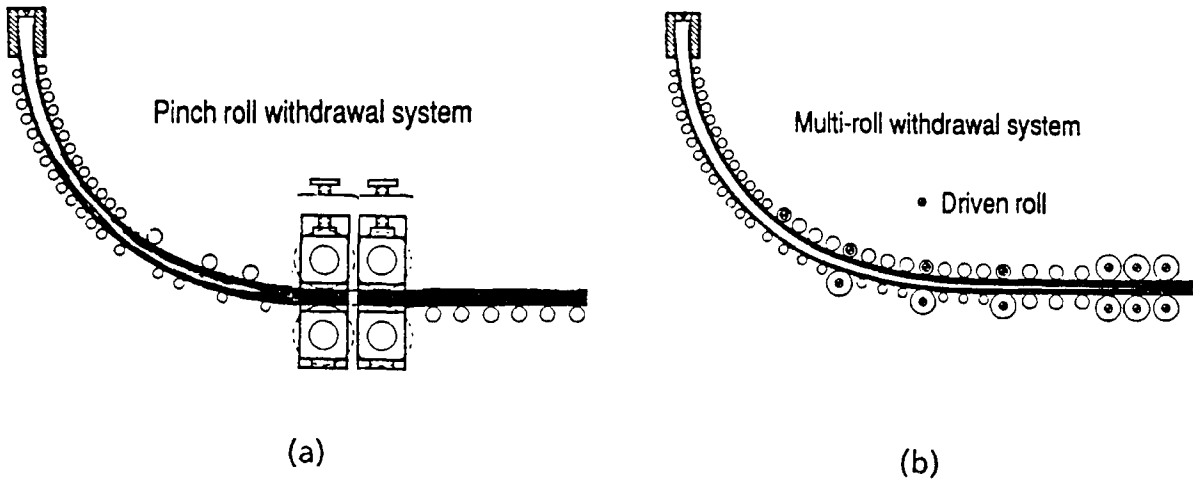


Figure 3.38 Strand withdrawal unit for (a) a bloom machine and (b) a slab machine.

still relatively thin and therefore the strains are usually not as high as when straightening with a liquid core. However, the same principles apply and many casters with straight moulds use multi point bending to achieve the required radius whilst reducing the strain rates to avoid internal defects. In such cases misalignment of the bending rolls again requires to be minimised to reduce misalignment strains (see para 3.4.2)

### 3.3.3 Withdrawal Units

The strand needs to be withdrawn from the machine under constant and controlled conditions and sufficient power and traction needs to be applied to achieve this. The withdrawal force has to be sufficient to overcome the frictional forces acting on the strand. These can arise due to:

- strand friction in the mould,
- friction of the support rolls in their bearings resulting from their operating loads,
- rolling friction owing to strand bulging between the rolls.

It should also be noted that the dead weight of the strand itself acts in favour of reducing the required withdrawal force.

Figure 3.38 shows examples of withdrawal units for a bloom machine and a slab machine.

Modern withdrawal units for slab machines are multi roll withdrawal systems, the traction and power being distributed over several roll pairs. The drive roll pairs achieve the correct amount of traction by the use of hydraulic forces slightly in excess of the ferrostatic force at that position. The withdrawal forces occurring in slab machines can only be overcome by the multi roll withdrawal system. Such a system successfully reduces the strand withdrawal force at an early stage, reducing it to a low level as the strand progresses through to caster. In Figure 3.39, Curve (a) represents the tensile force pattern calculated for a slab measuring  $2000 \text{ mm} \times 205 \text{ mm}$  cast at a speed of  $0.8 \text{ m/min}$ .<sup>6</sup>

The tensile force just below the mould shows a slight initial decrease owing to the dead weight of this strand. It remains at the relatively low value until the strand reaches the straightening section where it abruptly increases in magnitude. Following complete solidification the rate of increase eases due to the elimination of ferrostatic forces. Curve (b) represents the sum of the tensile forces measured at the individual drives. The difference between the calculated and the measured force at the ends of the two curves, which indicate the total tensile force, constitutes the error between the calculated and measured values. This error amounts to about 10% and is due to the many assumptions made. Curve (c) represents the

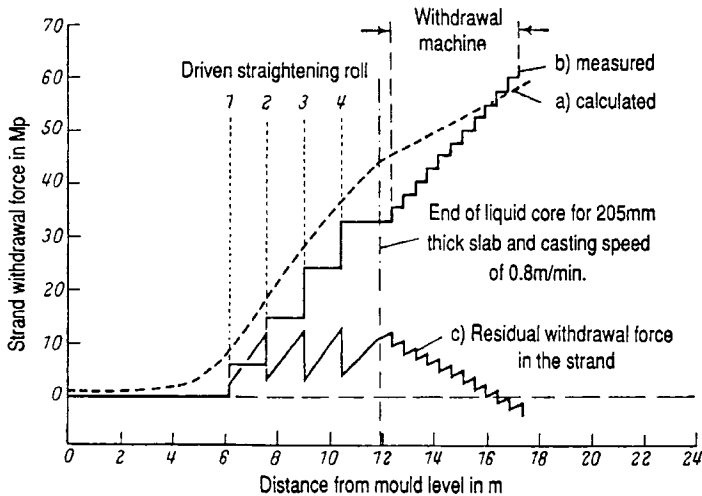


Figure 3.39 Measured and calculated strand withdrawal forces in a bow-type caster with four straightening points.

tensile forces remaining in the strand after application of the withdrawal forces and, as such, indicates the loading to which the strand is subjected during the withdrawal process. This curve was determined from the difference between the values represented by curves (a) and (b). The negative withdrawal force value indicates that the strand is being pushed and thus no longer subjected to tensile forces.

### 3.4 Computer Simulation Models

There are many computer models which have been developed for various aspects of the continuous casting process. These include:

- Liquid steel temperature model in the ladle and tundish (described briefly in Section 2.3)
- Fluid flow models of tundish and mould
- Powder feed model (see Section 3.1.2)
- Temperature distribution in the mould copper plates (see Section 3.1.2.5)
- Strand Solidification Model.
- Strand Bulging Models
- Roll temperature Distribution and Deflection Models

This chapter will only deal with the solidification model, the strand deformation models and the roller temperature and deflection models all of

which depend entirely on the data which have been acquired and described in Sections 3.1, 3.2 and 3.3.

### 3.4.1 The Strand Solidification Model

The strand solidification model<sup>21</sup> developed over many years in British Steel tracks a rectangular section normal to the axis of the strand and solves numerically by the finite difference method the Fourier equation for heat diffusion subject to the time dependent boundary conditions encountered by the section as it passes down the strand. The Fourier equation is:

$$\frac{\partial^2 T}{\partial x^2} + \frac{\partial^2 T}{\partial y^2} + \frac{\partial^2 T}{\partial z^2} = \frac{\rho c}{K} \frac{\partial T}{\partial t}$$

where  $x, y$  and  $z$  are the cartesian co-ordinates  
 $T$  is the temperature in °C at the point  $x, y, z$   
 $\rho$  = density (Kg/m<sup>3</sup>)  
 $c$  = specific heat (J/Kg K)  
 $K$  = thermal conductivity ( W/mK)  
 $t$  = time (s)

The data for  $\rho$ ,  $c$  and  $K$  are all included in the model as functions of temperature. It has been shown<sup>22</sup> that the high lateral heat fluxes produced by the mould, spray, rollers and radiative cooling (i.e. in the  $x$  and  $y$  directions) allow a two dimensional treatment to be valid since conduction along the strand axis ( $z$  direction) is negligible. Therefore the  $\partial^2 T / \partial z^2$  can be eliminated.

For all practical purposes the cooling is symmetrical about the mid vertical planes of the wide and narrow faces. Therefore only one quarter of the strand section is considered. This results in the saving of time for each simulation run.

Details of the early developments of this model were first published in 1975<sup>21</sup> and therefore considerable further developments have occurred over the intervening time. More importantly however, is the accumulation of the vast amount of measured data (as described in Sections 3.1, 3.2 and 3.3) which enables relative and accurate boundary conditions to be used in the solution of the basic Fourier equation. This means that at each position as the section travels down the strand heat fluxes can be applied and which can vary around the periphery of the section. At the solidification front the latent heat ( $L$ ) liberated on solidification is dealt with by essentially multiplying the calculated temperature differential by the ratio  $c/(c+L)$  in the solidus/liquidus region for the appropriate mesh points in the finite difference calculation procedure. The mixing in the liquid steel is

accounted for by the use of an increased thermal conductivity in this region.

The running of this model enables temperature distributions within the tracked section to be computed at each position down the strand. Printouts, therefore, of temperature profiles down the strand can be obtained at any position around the periphery. The shell thickness as a function of distance from the meniscus (of the liquid metal in the mould) can be readily obtained. This represents the solidus isotherm. Figure 3.40 shows an example of shell thickness (solidus isotherm) for a 240 mm slab soft cooled and cast at 0.8 m/min. Also included is a plot of the liquidus isotherm.<sup>19</sup>

The region between the liquidus and solidus isotherm is partly liquid and partly solid and is termed the 'mushy' zone. The 40% and 70% solid fraction positions are also shown.

Figure 3.41 shows the temperature profile down the mid broad face of a 1830 mm × 230 mm C/Mn slab cast at a speed of 0.8 m/min. The secondary cooling sprays for this simulation extended to 17.5 metres down the strand on the broad face and the specific water consumption was 0.35 L/Kg.

It should be noted that the surface temperature during the contact of each roll drops by about 100°C whilst, in this case, spray water effect is much less ('soft cooling').

The solidification model has been used extensively to design the secondary spray cooling systems on many casters to enable the conditions to

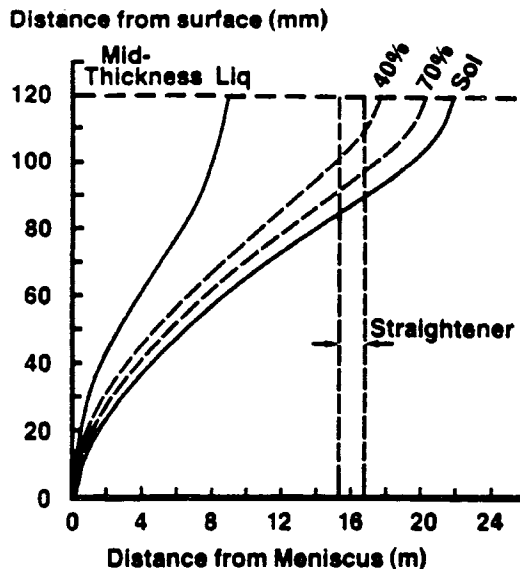


Figure 3.40 Solidus and liquidus isotherms for a 1100 × 225 mm slab.

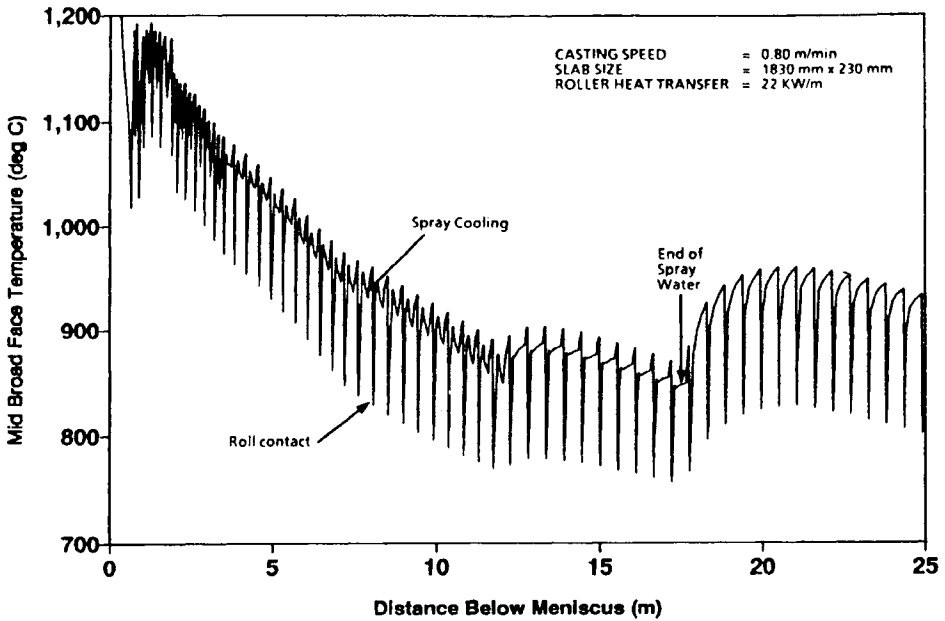


Figure 3.41 Surface temperature profile down the mid broad face for a 1830 mm  $\times$  230 mm slab.

be changed and controlled for various steel grades, with different steel grades requiring particular surface temperature patterns. This will be discussed more fully in Section 4.2.

### 3.4.2 Strand Deformation Model

During bloom and slab casting the ferrostatic pressure of liquid steel causes the strand to bulge between the guide rolls, resulting in strains at the solid/liquid interface, which can cause cracks to form, and which are penetrated with solute enriched liquid. The strength and ductility of steel decreases rapidly at the solid/liquid interface such that strains in the range 0.3–1.5% are sufficient to cause cracking. In addition to inter-roll bulging, strains arise in the solidifying shell as a result of roll misalignment, roll bending and strand straightening. Increasing the roll pitch results in an increase in bulging and an increase in bulging strain. However, strains due to the same roll misalignment decrease with increasing roll pitch. There is therefore an optimum roll spacing which minimises the combined bulging and misalignment strains.

To enable the solid/liquid interface strains to be calculated there is a need to be able to calculate the amount of inter-roll bulging and the curvature of the outer surface of the strand in the casting direction.

The temperature distribution within the solidified shell is calculated using the solidification model described above for the appropriate casting speed and cooling conditions.

Finite element models<sup>23</sup> have been developed to calculate the inter-roll bulging, bulging strain and misalignment strains. These models use the output from the solidification model to define the temperatures together with measured creep properties for the particular steel grade.

The following gives a brief description of the principles used in the bulging and strain calculation models.

Slab movement is simulated in the model by a mechanism of shifting columns of elements, with their associated viscoplastic strains and displacements, in the casting direction such that a column of elements leaving one roll position will effectively travel a complete roll pitch to the next roll. This is achieved by arranging columns of elements of equal width in the model such that the time to travel one element length  $t_e$  is given by

$$t_e = L/VN$$

where  $L$  = roll pitch

$N$  = number of columns of element

$V$  = casting speed

The slab shell is allowed to creep in increments  $\Delta t$  for a total time  $t_e$  after which the viscoplastic strains and displacements for each column  $i$  are transferred into columns  $i + 1$  and a column of elastic elements are substituted into column 1 (see Figure 3.42). The column of elements moving into the  $N$ th column, however, will have displacements which result in the surface of the slab moving inside the roll. This displacement into the roll is

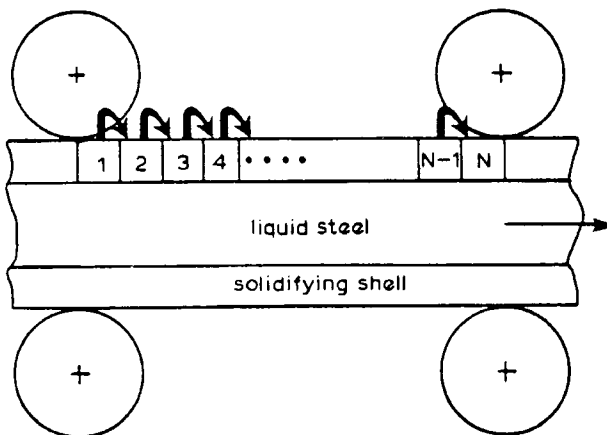


Figure 3.42 Simulation of slab movement.

Table 3.2 Comparison of calculated and measured inter-roll bulging

Roll pitch (mm)	Measured bulge (mm)	Calculated bulge (mm)
430	0.4– 1.6	0.36
860	5.0– 4.0	6.9
1290	35.6–42.0	46.2

gradually reduced to zero, during the next time period  $t_e$  in proportion to the time increments  $\Delta t$  (incremental displacement techniques), such that at the end of the time period  $t_e$  the boundary conditions are satisfied and the slab comes into perfect contact with the roll.

Slab bulging calculations using the incremental displacement method, and measured creep material properties for 0.185% C steel,<sup>24</sup> have been compared with measurements of slab bulging.<sup>25</sup>

Measurements of slab bulging were made for three roll pitches by first removing one then two adjacent rolls to give roller spacings of 430, 860 and 1290 mm. Calculations of slab bulging for each of these roll spacings have been used as a check on the validity of the model calculations. The results given in Table 3.2 show good agreement between calculations and measurements.

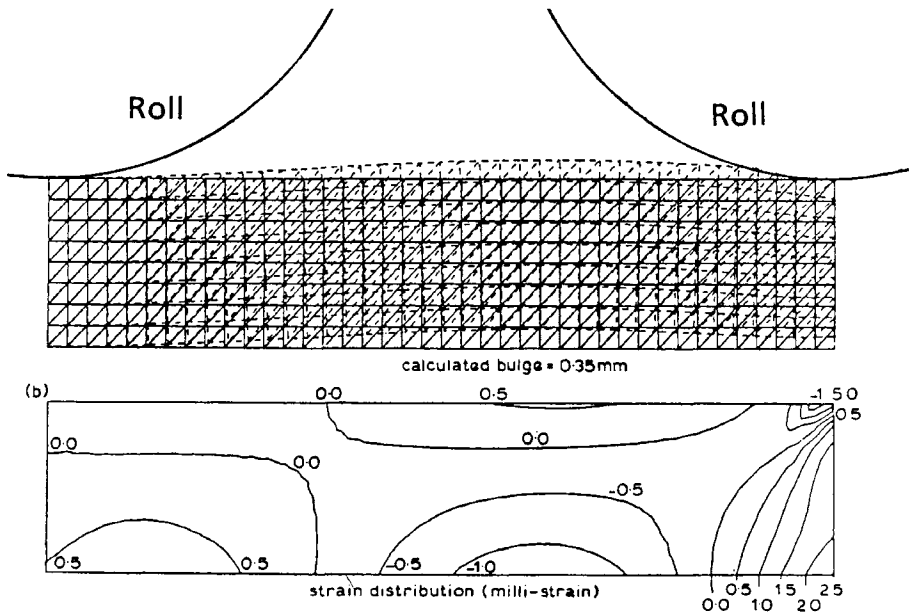


Figure 3.43 (a) Calculated slab bulging and (b) shell strain distribution 7 m from the meniscus: roll pitch 363 mm, shell thickness 77 mm and casting speed 0.8 m/min.

Model results used to analyse slab bulging and bulging strains for slabs cast on a 12.5 m radius machine with well designed roll pitches show that during normal operation slab bulging, and strains at the solid/liquid interface are small. A typical result is shown in Figure 3.43 where slab bulging at a distance of 7 m from the liquid metal level is calculated to be 0.35 mm and the resulting strain at the solid/liquid interface beneath the roll is calculated to be 0.25%.

However, strains at the solid/liquid interface can also be induced by misalignment of adjacent rolls or by one of the rolls becoming permanently bent. Normally the tolerance for the deviation of roll gaps is 0.5 mm for machines casting segregation sensitive grades.

In a particular machine the roll diameters and pitches vary down the machine. Figure 3.44 shows the calculated inter-roll bulging and consequent bulging strains for a typical slab casting machine using single piece rolls. The calculations have been carried out for

- a casting speed of 0.8 m/min with secondary cooling of 0.1 L/Kg
- a casting speed of 0.9 m/min with secondary cooling of 0.7 L/Kg

Whilst smaller roll pitches will reduce the strains due to inter-roll bulging they increase strains due to roll misalignment. Roll bending as described earlier, is only one reason for rolls deviating from the true pass line. Deviation can occur for the following reasons.

- roll eccentricity
- roll misalignment due to bearing wear or even failure
- roll wear
- segments not properly aligned with each other
- distortion of the segment frame due to mechanical and thermal loads.

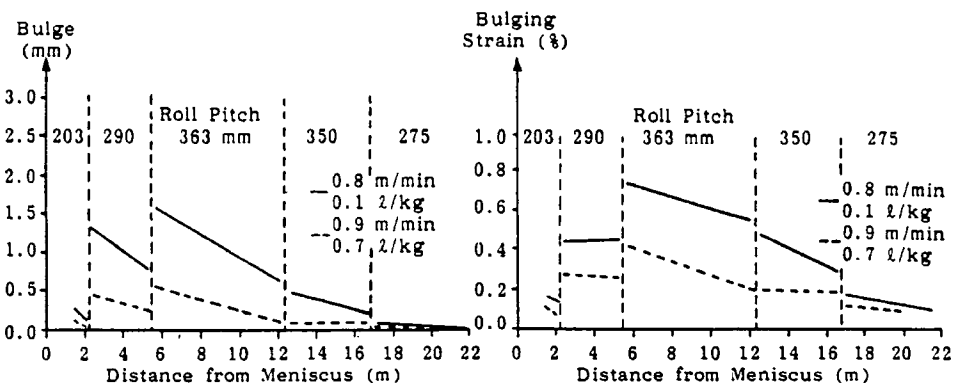


Figure 3.44 Calculated inter-roll bulging and bulging strains.<sup>19</sup>

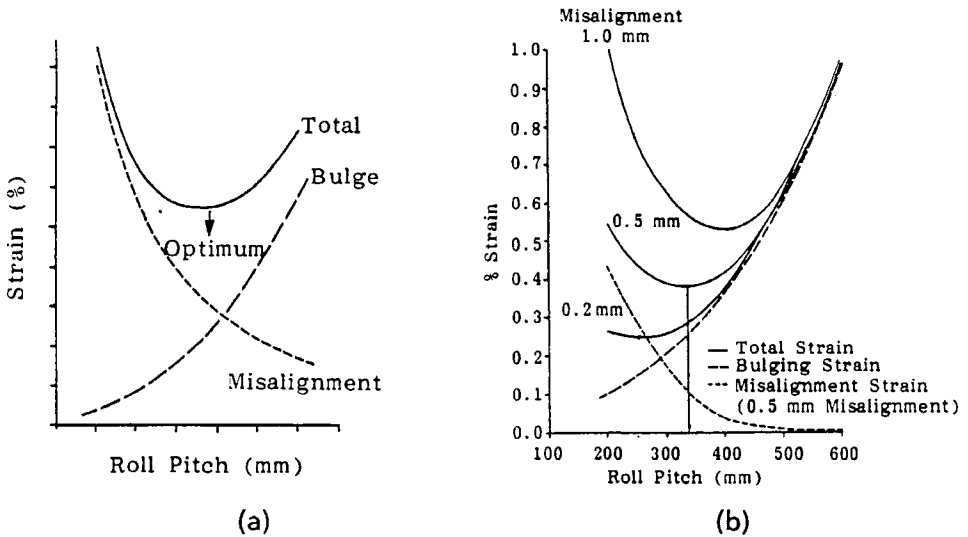


Figure 3.45 Calculation of inter-roll bulging and misalignment stresses showing (a) general principal of strain summation and (b) specific calculations for various misalignments.

Superimposed on the bulging strains, (shown in Figure 3.44) are strains caused by roll misalignment. Misalignment strains (for a given misalignment) are reduced by increasing the roll pitch and therefore an optimum roll pitch can be found which minimises the total strain resulting from bulging and misalignment as shown in Figure 3.45 (a). The influence of different assumed values of total roll misalignment on strains can be assessed as shown in Figure 3.45 (b) for each position down the caster.

The *total* strain at the solid/liquid interface is the critical issue in segment design. These can also be calculated using the models for particular roll misalignments. Additional strains are also induced when the strand is straightened.

Figure 3.46 gives an example of the calculations of the various strains at the straightener for a 240 mm thick slab cast at 0.9 m/min. This shows the bulging and misalignment strains as shown in Figure 3.45(b) but with the straightening strains at both the outer surface and the solid/liquidus interface included.

### 3.4.2.1 Critical Strain Levels

Critical strain levels (above which cracking occurs) depend on the products e.g. more strain is acceptable for most strip grades than for many plate grades for which the internal quality is more sensitive to different types of segregation. Therefore it may not always be necessary to incur the

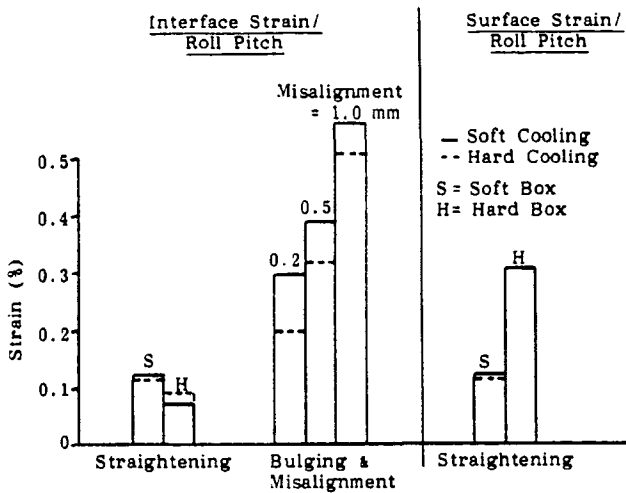


Figure 3.46 Calculated total strains during strand straightening.

expense of employing all possible means of reducing strains (e.g. split roll installation and maintenance costs). Critical strain levels are also affected by the rate of strain, since higher strain levels can be tolerated where the rate of strain is lower. Consequently, there is no simple answer to what is a tolerable strain level; indeed laboratory testing of slab samples would at first suggest higher strain levels could be tolerated than the levels which in practice give problems on casters; it is concluded that in casting there is a cumulative effect of strains at successive rolls.

### 3.4.3 Roller Temperature and Deflection Models

Finite element models have been developed<sup>26</sup> to calculate the temperature distribution and the amount of deflection which occurs due to mechanical and thermal forces and for various roller designs. Two main models were used. The first model is used to calculate the temperature distributions within the roller both during normal operation and during strand stoppages. This temperature information is then input into the second model which determines the amount of bending due to both the thermal loadings and that due to the mechanical loadings which are applied to the rollers by the strand ferrostatic pressure. Symmetry is assumed both for the rollers and the strand and Figure 3.47 shows the finite element mesh arrangement for the temperature modelling of the three types of rolls shown in Figure 3.30 i.e. centre bore, peripherally drilled and scrolled rolls respectively.

In this case all the rollers were single piece rollers with no centre support and were 310 mm in diameter. Figure 3.48 shows the finite element

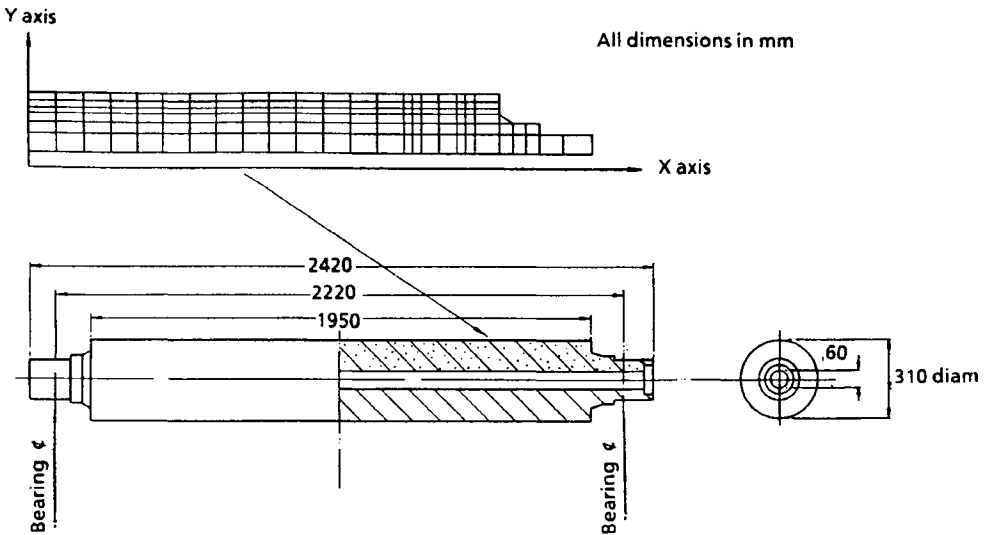


Figure 3.47 Finite element meshes used to determine temperature with various roller designs.

mesh arrangement used to determine roller bending from the thermal and mechanical loadings.

As outlined in Section 3.2.3 the stability of the roller geometry is an essential requirement to achieve good internal and surface quality and one of the most arduous situations for the rollers is when a strand stoppage occurs usually at ladle changeover or as a result of a breakout. In this case the thermal loading is increased very significantly due to the increased temperature gradient across the roll diameter. In these extreme cases the roller can become permanently bent and hence detrimental to maintaining a constant roll gap geometry. The roller models have been used extensively to support the experimental work described in Section 3.2.3 and Figure 3.49 shows how the models indicate the bending which occurs during a prolonged strand stoppage for the three different roller designs discussed earlier.

It should be pointed out that stoppages of this duration are very infrequent and the long duration of 40 minutes is mainly hypothetical in the course of the deformation studies. Any strand stoppages which do occur are usually less than 5 minutes and often result during ladle or tundish changing.

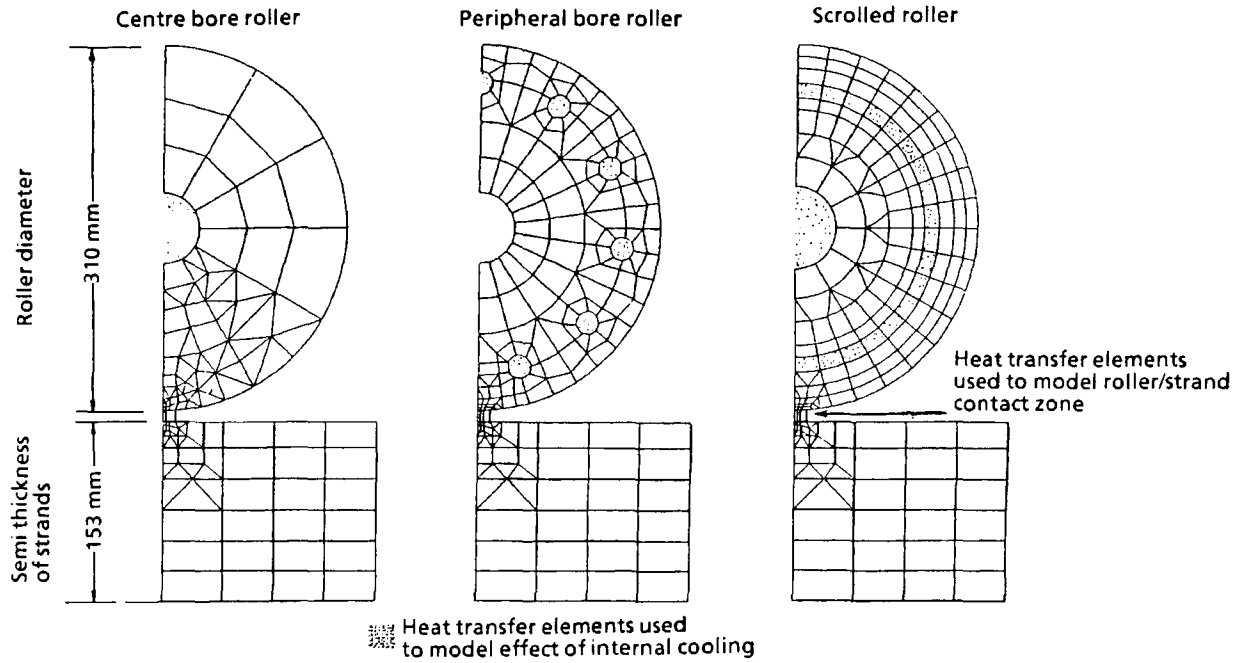


Figure 3.48 Axisymmetric finite element mesh used to determine roller bending due to thermal and mechanical loadings.

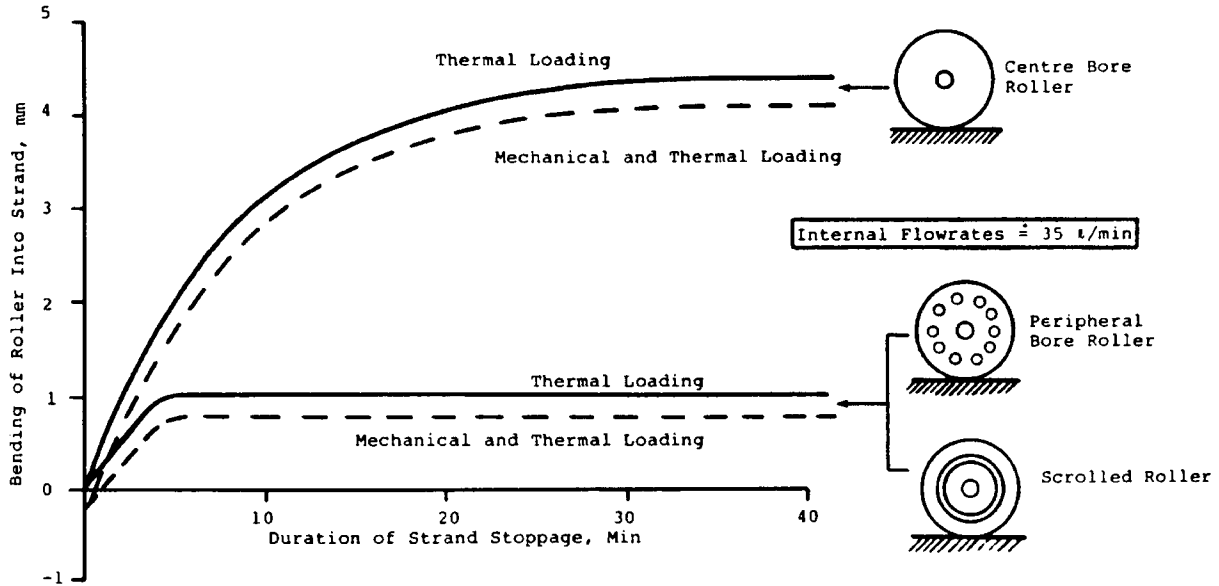


Figure 3.49 Comparison of predicted bending of different roller designs during a 40-minute stoppage.

## References

1. International Iron & Steel Institute, *Continuous Casting of Steel 1985 – A Second Study*.
2. T. Harabuchi, Summer Conference, University of Michigan, May 1984.
3. R. Pellikka and E. Rättyä, *Jernkontoret Ann.* 1980, 6, 52.
4. K. Tsutsumi *et al.*, 'Development of new high speed mould width changing during continuous casting,' *Continuous Casting '85*, London May 1985, Paper 66.
5. M. Yamahiro, T. Inoue and T. Yukawa, 'Variable width moulds in continuous casting' *AIME Open Hearth Proceedings*, 67, (1979), Detroit.
6. H. F. Schrewe, *Continuous casting of Steel* Verlag Stahleisen mbH, Dusseldorf, 1987.
7. W. R. Irving, 'Mould heat transfer,' *Concast Metallurgical Seminar on Slab Casting*, May 1976, (74), 51.
8. M. M. Wolf, 'Mould oscillation guidelines,' *AIME Steelmaking Conference Proceedings*, 1991.
9. S N Singh and K E Blazek: Heat transfer and skin formation in a continuous casting mould as a function of steel carbon content, *AIME Open Hearth Proc.*, 1974, 57, Atlantic City, 16.
10. A. Grill and J. E. Brimacombe, 'Influence of carbon content on rate of heat extraction in the mould of a continuous casting machine,' *Ironmaking and Steelmaking*, 1976, 3 (2), 76.
11. R.J. Gray, A. Perkins and B. Walker, 'Quality of continuous cast slabs,' *Proc. Metal Society*, Sheffield, July 1977, 300.
12. International Iron and Steel Institute, *A study of the Continuous Casting of Steel*, Brussels, 1977.
13. E. Mizikar, 'Spray cooling investigation for continuous casting billets and blooms,' *Iron and Steel Eng.* 1970, 53.
14. A. Etienne and B. Mairy, 'Heat transfer in continuously cast strands,' *CRM Report No.35*, November 1979.
15. H. Muller and R. Jestler, 'Untersuchung des Wörmeü bergenges an einer simulierten Sekundörkühlzone beim Stranggiessverfahren. Arch Eisechüt-tansen, 1973, 44 (8), 589.
16. G. Kaestle, H. Jacobi and K. Wünnenburg, 'Heat flow and solidification rate in strand casting of slabs,' *AIME Steelmaking Proc.*, 1982, 65, 251.
17. A. Perkins, M. G. Brooks and R. S. Haleem, Roll performance in continuous slab casting, *Continuous Casting '85*, London, Paper 67.
18. W. R. Irving, A. Perkins and M. G. Brooks, 'Effect of chemical, operational and engineering factors on segregated and continuously cast slabs,' *Ironmaking & Steelmaking*, 1984, 11 (3).
19. B. Patrick, B. Barber, D. J. Scoones, J. L. Heslop and P. Watson, 'The evaluation of schemes for upgrading continuous steel casting facilities,' *1st European Conference on Continuous Casting*, Florence, Italy, Sept 1991, 1.111.
20. A. Vaterlaus, 'Finite element analysis for slab straightening with a liquid core,' *Trans. ISIJ*, 1983, 23, (7), B-242.
21. A. Perkins and W. R. Irving, 'Two-dimensional heat transfer model for continuous casting of steel,' *Mathematical process models in iron and steelmaking*, 187-199, The Metals Society, 1973, 187-199.

22. A. W. Hills, *Institute of Chemical Engineers Symposium on Chemical Engineering in Metallurgical Industries*, 1963, 128.
23. B. Barber, B.A. Lewis and B. M. Leckenby, 'Finite Element analysis of strand deformation and strain distribution in solidifying shell during continuous steel casting, *Ironmaking and Steelmaking*, 1985, **12** (4), 171.
24. A. Palmaers and A. Etienne, *Coulée et solidification de l'acier*, Final Report Annexe III Convention, CCE/CRM 6210-50/2/201 Liege, Belgium, 1977.
25. K. Wünnenberg and J. Dubendorf, 'Strand bulging between supporting rollers during continuous slab casting,' *Stahl und Eisen*, 1978, **98**, 254.
26. J. McCann and P. G. Stevens, 'Evaluation, development and design of transport rollers in continuous casting plant,' Commission of the European Communities, Final Report No. EUR 9813, EN.